Modeling the impact of lane-changing's anticipation on car-following behavior

Chen, Kequan; Knoop, Victor L.; Liu, Pan; Li, Zhibin; Wang, Yuxuan

DOI
10.1016/j.trc.2023.104110

Publication date
2023

Document Version
Final published version

Published in
Transportation Research Part C: Emerging Technologies

Citation (APA)
Chen, K., Knoop, V. L., Liu, P., Li, Z., & Wang, Y. (2023). Modeling the impact of lane-changing's anticipation on car-following behavior. *Transportation Research Part C: Emerging Technologies*, *150*, Article 104110. https://doi.org/10.1016/j.trc.2023.104110

Transportation Research Part C 150 (2023) 104110

Contents lists available at ScienceDirect

Transportation Research Part C

journal homepage: www.elsevier.com/locate/trc

Modeling the impact of lane-changing's anticipation on car-following behavior

Kequan Chen [a], Victor L. Knoop [b], Pan Liu [a,*], Zhibin Li [a], Yuxuan Wang [a]

[a] Department of Transportation, Southeast University, Southeast University Road #2, Nanjing 211189, China
[b] Civil Engineering of Technology, Delft University of Technology, Stevinweg 1, Delft 2628CN, the Netherlands

ARTICLE INFO

Keywords:
Car-following model
Lane-changing impact
Anticipation
Trajectory data

ABSTRACT

Lane-changing (LC) in congested traffic has been identified as a trigger for the sudden deceleration behavior of the new follower in the target lane, leading to severe traffic disturbances. Thus, investigating the response of the new follower to an LC maneuver is an important research topic in the literature. To date, numerous efforts have been devoted to understanding the impact of the lane changer on the new follower after the insertion, while less attention has been given to this influence during the pre-insertion stage (anticipation). Therefore, this paper aims to establish a new car-following (CF) model to capture the new follower's driving behavior during anticipation. Specifically, we introduce an attention mechanism deviating from Newell's CF rules to quantify the impact of anticipation. Then, we apply a neural network with an attention layer to estimate the attention mechanism and incorporate it into the Newell CF model, which yields a new CF model, denoted as CF_Attention. Using real-world trajectory data, we design three experiments and select three representative CF models to validate the CF_Attention. The results indicate that the CF_Attention outperforms the other models in predicting the new follower's trajectory, which is not affected by the heterogeneous behavior of the new follower and the anticipation duration. Additionally, the CF_Attention is proven effective in capturing the speed-space relationship and the formation of oscillation. Finally, our transferability test suggests that the CF_Attention is promising for different locations and times without requiring retraining. The results of this study could advance the integration of the LC impact and CF behavior, and could be implemented into commercial traffic simulation programs to describe vehicle movements in traffic flow more accurately.

1. Introduction

In congested flow, lane-changing (LC) is one of the fundamental and crucial driving tasks that can lead to several important traffic problems, such as capacity drops (Laval and Daganzo, 2006), oscillations (Zheng et al., 2011), and increasing trend of traffic crashes (Li et al., 2020). The underlying cause of these negative issues during LC is the affected car-following (CF) behavior of surrounding vehicles. Among these vehicles, the immediate follower in the target lane (new follower) has garnered increasing interest because it directly responds to the LC maneuver. For example, an overreaction by the new follower during LC may induce a deceleration wave

* Corresponding author.
E-mail addresses: chenkequan@seu.edu.cn (K. Chen), v.l.knoop@tudelft.nl (V.L. Knoop), liupan@seu.edu.cn (P. Liu), lizhibin@seu.edu.cn (Z. Li), wangyuxuan@seu.edu.cn (Y. Wang).

https://doi.org/10.1016/j.trc.2023.104110
Received 27 October 2022; Received in revised form 14 March 2023; Accepted 16 March 2023
Available online 30 March 2023

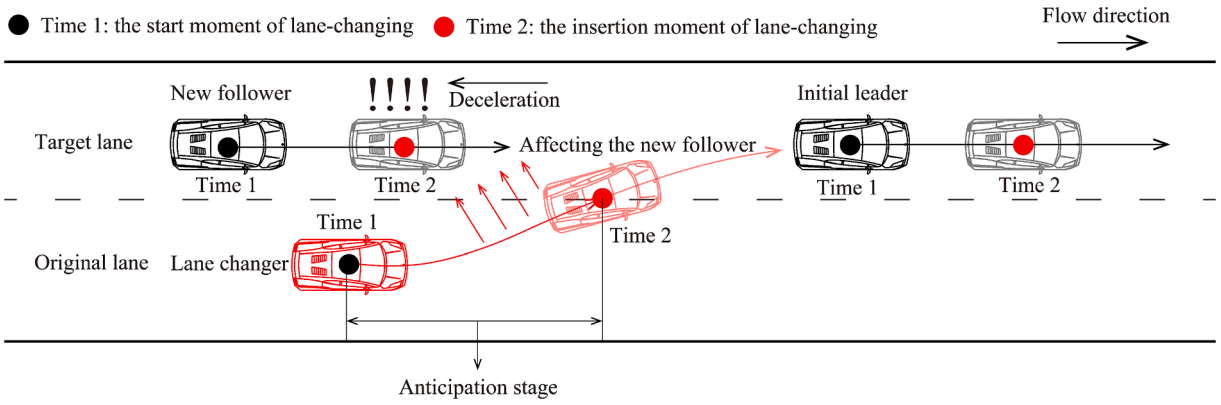

Fig. 1. Illustration of an anticipation process.

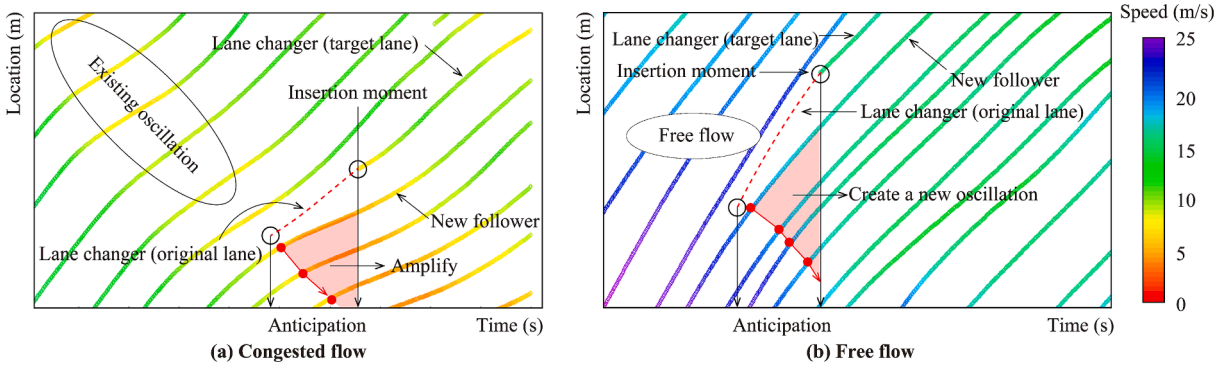

Fig. 2. The impact of anticipation on the driving behavior of the new follower.

that propagates upstream. Therefore, developing a precision CF model for the new follower during LC is appealing since it could facilitate an in-depth understanding of LC-related issues and set the stage for a more accurate micro-simulator.

Generally, a complete LC maneuver goes through two stages: (1) Anticipation: the lane changer remains in its original lane while making preparations to move to the target lane; (2) Relaxation: the lane changer successfully enters the target lane and gradually follows its new leader steadily (Zheng et al., 2013). Given that the relaxation stage has been considered as the primary cause of capacity drops, considerable research has been conducted to incorporate the impact of relaxation into CF models to reproduce such negative traffic phenomena. Regarding the anticipation stage, readers are referred to Figs. 1 and 2 for clear illustrations of its process and the impact on the new follower, respectively. Note that Fig. 1 displays three vehicles at two continuous time points labeled "Time 1" and "Time 2", representing the start and insertion moments of LC, respectively. For brevity, these three vehicles are denoted as "new follower", "initial leader", and "lane changer" throughout this paper. As shown in Fig. 1, the lane changer first indicates the intention of changing lanes with the new follower. If the initial gap in the target lane is not large enough for a safe insertion, the new follower may be forced to decelerate to enlarge the gap. This deceleration behavior may cause a significant impact on the traffic flow by either amplifying the existing oscillation (Fig. 2**(a)**) or creating a new oscillation (Fig. 2 **(b)**).

Although some recent empirical studies have also reported similar negative impacts of anticipation on the new follower's behavior (Yang et al., 2019a; Chen et al. 2022), relatively limited attention has been paid to quantifying these impacts. As a result, there is currently a lack of clarity regarding a CF model that can accurately describe the new follower's behavior during anticipation. Naturally, this raises three interrelated questions: (a) Whether existing CF models, which do not account for the impact of anticipation, can accurately estimate the new follower's trajectory during anticipation; (b) How to formulate the impact of the lane changer on the new follower; (c) Whether a new CF model incorporating this anticipation impact formulation can effectively reproduce the new follower's behavior during anticipation.

To address the research questions above, we formulate the new follower's behavior by considering the perception of space headway during anticipation and incorporate it into the Newell CF model, which forms a new CF model. The main contributions of our study are summarized as follows:

(1) We propose an attention mechanism to describe the new follower's response to the anticipation stage. This mechanism consists of two attention weights representing the new follower's attention on the initial leader and the lane changer. They are derived from Newell's CF rule based on the difference between the desired space headway of the new follower and the actual values with its initial leader and the lane changer. This approach can be easily extended to the existing CF models.

(2) We develop a neural network with an attention layer to predict the new follower's attention mechanism. This network is trained and tested with real-world trajectory data and performs fairly well. The outcomes of the neural network are incorporated into Newell's CF model, yielding a novel CF model. It is the first attempt to model the new follower's behavior by considering the impact of the anticipation stage of LC from a nuanced perspective, which sheds light on the integration of the CF model and LC impact.

(3) We carefully design three experiments to demonstrate the performance of the new CF model in terms of trajectory, speed-space relationship, and oscillation. We also compare our model with three widely accepted CF models: (1) Newell's CF model (Newell, 2002), (2) Modified Newell's CF based on the idea of Hidas (Hidas, 2002), and (3) The CF model proposed by Laval and Leclercq (2008). The tests show that the new CF model significantly improves prediction accuracy. The transferability tests demonstrate that this model can be directly applied to other locations and times.

The rest of this paper is organized as follows. Section 2 provides a comprehensive literature review. Section 3 explains the construction procedure of the new CF model, including the formulation of the anticipation impact, the attention neural network, and the simulation steps for the new CF model. Section 4 illustrates the empirical data. Section 5 presents the training and testing results of the attention neural network. Section 6 designs three experiments and compares the simulation results between the new CF model and three investigated CF models. Section 7 gives the transferability test results of the new CF model. Section 8 concludes our work and offers suggestions for future research directions.

2. Relevant literature

In this section, we present a comprehensive review of previous studies on the impact of LC anticipation on the new follower's behavior and the data-driven CF model, which are relevant to our work.

2.1. Impact of lane-changing anticipation

Previous studies on the impact of LC anticipation on the new follower's driving behavior can be mainly categorized into modeling and empirical investigation studies.

To reproduce the trajectory of the new follower during anticipation, many studies have proposed and incorporated different assumptions into basic CF models, such as those by Newell (2002) and Treiber et al. (2000). For instance, Hidas (2002) assumed that the new follower would treat the lane changer as the following target once the lane changer decides to change lanes. He added this assumption to the Simulation of Intelligent TRAnsport Systems and found that the flow-speed relationship in congested flow could be generated only when this assumption is considered. On the other hand, Yeo et al. (2008) suggested that the new follower follows either the initial leader or the lane changer during anticipation. To reflect this following behavior, they relaxed the jam gap and reaction time in the Newell CF model with two fixed constant values. The new CF model is validated using CF trajectory and aggregate data from loop detectors. Schakel et al. (2012) assumed that the new follower would enlarge the gap in the target lane if the required deceleration of the new follower is less than the safe deceleration threshold. They incorporated this cooperation behavior of the new follower into the intelligent driver model, which has been validated using speed and flow patterns. More recently, Keane and Gao (2021) observed that the new follower's behavior predicted by existing CF models is more likely to exhibit a radical reaction to the sudden jump in headway caused by the LC insertion. To mitigate this unrealistic issue, they proposed a relaxation model to smooth the changing process of space headway, which could be easily integrated into the parametric or nonparametric CF models.

Now, we focus our attention on the empirical investigation studies in terms of the new follower's reaction to anticipation. Heesen et al. (2012) concluded that the new follower's willingness to decelerate to provide an available gap depends on the driving behavior when the lane changer sends an LC request. Using real-world vehicle-level trajectory data, Yang et al. (2019b) examined 5339 LC trajectory samples and found that approximately 44% of new followers would decelerate when they noticed the LC motivation in the adjacent lane. Chen et al. (2022) investigated the impact of anticipation on the new follower and found evidence of its significance. To this end, they developed two binary logit models, demonstrating that including the anticipation-related factors significantly improved the prediction accuracy regarding whether the new follower changes its driving behavior during anticipation. These findings highlight the importance of considering the anticipation impact when studying the behavior of the new follower.

The studies mentioned above have either developed CF models with assumptions that have yet to be empirically justified or only reported the negative impacts of the anticipation on CF behavior. As a result, a new CF model incorporating these empirical findings is needed to predict the new follower's trajectory realistically. One notable study to tackle this issue was proposed by Zheng et al. (2013), who investigated the NGSIM trajectory data and found that the LC anticipation is more likely to induce the new follower to deviate from its equilibrium state. They further suggested that the new follower's behavior during anticipation is not significantly different from that during relaxation. Thus, the relaxation-related model (Laval and Leclercq, 2008) could also potentially capture the new follower's reaction behavior during anticipation. However, this conjecture remains to be validated, which will be tested in this paper.

Regarding the relaxation-related model, Laval and Leclercq (2008) constructed a relaxation parameter to reflect the new follower's willingness to accept the speed differences during relaxation. They incorporated this parameter into the CF rules of Laval and Daganzo (2006) to reproduce the new follower's deviation behavior. This new CF model has been validated by comparing the predicted oblique queueing diagrams with the observed ones. After that, Duret et al. (2011) adopted the measurement of passing rates proposed by Chiabaut et al. (2009) to explain the relaxation phenomenon. They derived an alternative formulation, which is strictly equivalent to the work of Laval and Leclercq (2008), and incorporated it into the Newell CF model to evaluate the impact of anticipation on traffic streams.

2.2. Hybrid CF models

In recent years, the availability of high-quality trajectory data and advancements in artificial intelligence have led to a growing popularity of data-driven approaches for modeling CF behavior. These approaches offer two significant advantages over traditional models. First, they are more flexible as they can incorporate additional parameters affecting CF behavior. Second, they can effectively learn the patterns and rules of human driving from trajectory data, thereby improving prediction accuracy. Various data-driven models have been proposed to estimate CF behavior. For example, Zhou et al. (2017) proposed a CF model based on a recurrent neural network (RNN) to predict the traffic oscillation caused by asymmetric driving behavior, outperforming the classical CF model (Treiber et al., 2000). Huang et al. (2018) developed long short-term memory neural network (LSTM-NN) based CF model that captures driving characteristics in terms of hysteresis, discrete behavior, and intensity difference. The performance of this model has been demonstrated through comparison with other RNN-based CF models. Zhu et al. (2018) used deep reinforcement learning and a reward function based on the disparity between simulated and observed speed to reproduce CF behavior, resulting in improved accuracy over both traditional and recent data-driven CF models. Zhang et al. (2019) utilized LSTM to model CF and LC behaviors simultaneously. Ma and Qu (2020) proposed a sequence-to-sequence based CF model to handle the memorization of historical information and make multi-step predictions.

However, the above-mentioned data-driven CF models belong to "black box" making it difficult to explain the physical meaning and apply them directly in practice. In contrast, traditional physical-based CF models have distinct parameters with obvious physical meanings. Thus, the outcomes of these models are easily comprehended and controlled. To leverage the strengths of physical-based models and data-driven approaches, several hybrid CF models have been developed recently to mimic driving behavior. Yang et al. (2019a) discovered that combining the outcomes of the Gipps CF model and the Back-Propagation Neural Networks CF model can enhance the safety and robustness of CF trajectory control. Lee et al. (2019) applied the stochastic CF framework of Ngoduy et al. (2019) to estimate CF trajectory in multiple lanes, with the LC probability parameter predicted by Convolutional Neural Network. Mo et al. (2021) used mathematical models to generate additional unobserved driving data to improve the performance of two representative neural network models. Zhang et al. (2022) employed a neural process to calibrate the time-varying parameters in the Intelligent Driver Model. Given the advantages of hybrid models, in this study, we apply neural networks to predict the impact of anticipation and incorporate it into the Newell CF model to reproduce the new follower's trajectory during anticipation.

3. Methodology

In this section, we aim to address two challenges:

- How to formulate the behavior of the new follower under the coupled effect of the initial leader and the lane changer during anticipation (Sections 3.1 to 3.3)?
- How to develop a new CF model by incorporating the affected behavior of the new follower (Section 3.4)?

To achieve our goals, we first briefly review the CF model proposed by Newell (2002) to describe the driving behavior of the new follower (Section 3.1). Next, we propose the attention mechanism in Section 3.2 to quantify how the new follower's perception of spacing in front is affected during anticipation. Given that the attention mechanism is supposed to reflect the new follower's real behavior, the challenge lies in predicting it. Thus, in Section 3.3, we propose a neural network with an attention layer to cope with this issue. After that, we introduce the new CF model by incorporating the outcomes of the neural network into the Newell CF model (Section 3.4). To demonstrate the performance of the new CF model, Section 3.5 introduces three existing CF models for comparison.

3.1. Driver's following behavior

In this study, we adopt the CF model proposed by Newell (2002) as the basis of our new CF model. There are three reasons for using the Newell CF model rather than other CF models. First, the Newell CF model is capable of comparing theoretical jam spacing and reaction time with the real values, making it ideal for observing and predicting the deviation behavior of the vehicle. This feature has enabled it to be successfully utilized to investigate whether the lane changer affects the new follower in previous studies by Zheng et al. (2013) and Chen et al. (2022). Second, the Newell CF model has shown flexibility by being extended and modified in previous studies to predict CF behavior in various scenarios. Moreover, the separate item for space headway makes it easy to incorporate the attention mechanism established in Section 3.2. Third, as stated earlier, two classical CF models (Hidas, 2002; Laval and Leclercq, 2008) have integrated the LC impact into the Newell CF model. Considering these two models are selected as comparison benchmarks in our study, using the same base model allows a fair evaluation of the importance of the attention mechanism.

In the Newell CF model, the theoretical trajectory of the new follower is obtained by shifting the initial leader's trajectory with a response time lag τ and a stop distance lag d. Let i as the new follower, i-1 as the initial leader, and j as the lane changer in the adjacent lane. The mathematical formulation for predicting the new follower's trajectory is as follows:

$$x_i(t+\tau) = \min\left(v^{free}\tau + x_i(t), \max(\Delta S(t), 0) + x_i(t)\right) \tag{1}$$

where $x_i\,(t+\tau)$ is the location of the new follower i at time $t+\tau$, v^{free} is the speed limit, and $\Delta S(t)$ is the congested moving term, which can be calculated as **Eq. (2)**:

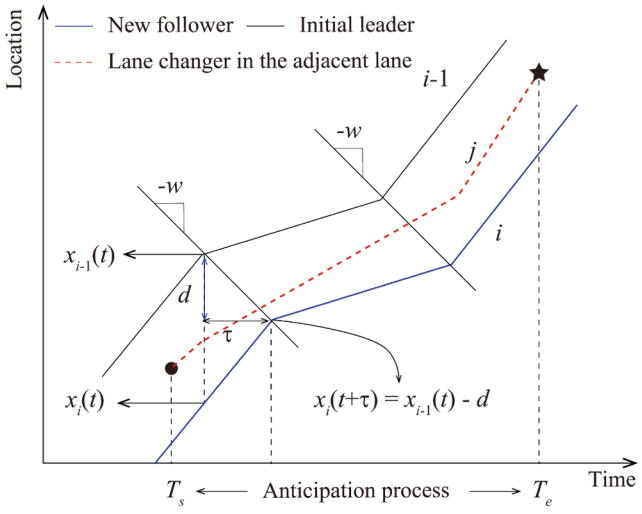

Fig. 3. Framework of the CF_Newell.

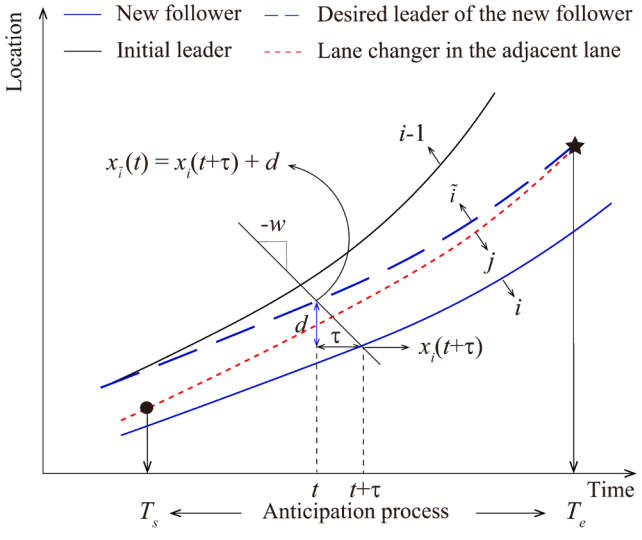

Fig. 4. Formulation of the desired leade's trajectory.

$$\Delta S(t) = x_{i-1}(t) - x_i(t) - d \tag{2}$$

where $x_{i\text{-}1}$ (t) is the location of the initial leader i-1 at time t.

Fig. 3 shows a typical example where the new follower i follows the rules of **Eqs.** (1) and (2) (abbreviated as CF_Newell). Let T_s and T_e as the start and end moments of the anticipation process, respectively. In this example, the lane changer j in the adjacent lane initials its anticipation process at time T_s. The red dotted line represents the lane changer's trajectory in the original lane. Since the lane changer's movement and its impact have not been considered, the trajectory of the new follower (shown as the blue line in Fig. 3) from T_s to T_e is obtained by shifting the initial leader's trajectory along the traffic wave w.

The ratio of the actual response time to the equilibrium time is applied to measure the new follower's driving behavior, which can be expressed as follows (Chen et al., 2012):

$$\eta_i(t) = \tilde{\tau}_i(t)/\tau \tag{3}$$

where $\tilde{\tau}_i(t)$ is the actual wave travel time at time t.

The time-dependent value of η_i (t) describes the new follower's response relative to the equilibrium during the anticipation process. We then measure the changing magnitude of η_i after the new follower i experiences an anticipation, denoted by $\Delta\eta_i$.

$$\Delta\,\eta_i = \eta_i(T_e) - \eta_i(T_s) \tag{4}$$

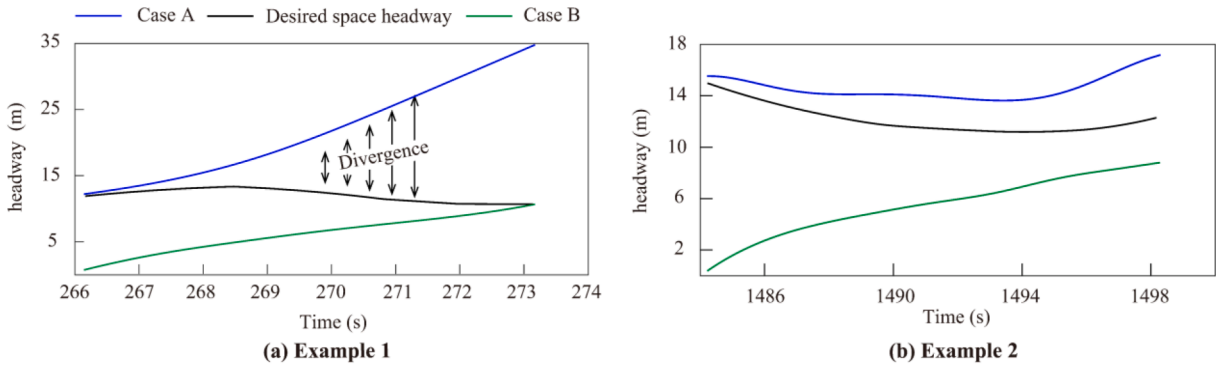

Fig. 5. The changing process of the real desired space headway in two examples.

Similar to the previous study (Chen et al., 2014), a threshold of 0.1 for $\Delta\eta_i$ is defined to classify the driving style of the new follower. The threshold of 0.1 is chosen because it is indicative of slight changes in the driver's reaction pattern that are considered the driver's inherent nature. Therefore, $\Delta\eta_i$ greater than 0.1 represents the new follower deviating from its leader. In this case, we categorized the new follower's style as defensive. In contrast, $\Delta\eta_i \leq 0.1$ represents the new follower closing to its leader, which can be categorized as aggressive.

3.2. Formulation of the new follower's response

In this section, we discuss how to formulate the new follower's response during anticipation. We first make an assumption that the new follower's movement is only limited by the initial leader and the lane changer. Then, we introduce a desired leader $\widetilde{i}$, which is a virtual product that describes the new follower's real CF behavior under the coupled effect of the initial leader and the lane changer. For the sake of simplicity, we also assume that the desired leader is the one the new follower would like to follow based on the Newell CF model rules. Thus, we can obtain the desired leader's trajectory by shifting back the new follower's real trajectory along with a negative response time ($-\tau$) and a negative stopped distance ($-d$); see Fig. 4 for an illustration. The desired leader's trajectory in congested moving term can be described by:

$$x_{\widetilde{i}}(t) = x_i(t+\tau) + d \tag{5}$$

where $x_{\widetilde{i}}(t)$ is the location of the desired leader $\widetilde{i}$ at time t.

According to **Eq.** (5), the new follower's desired headway can be calculated as $\Phi_i(t) = x_{\widetilde{i}}(t) - x_i(t)$. Here, we present two extreme cases to explain the construction idea of $\Phi_i(t)$:

- Case A: the new follower follows the initial leader ($\Phi_{A,i}(t) = x_{i\text{-}1}(t) - x_i(t)$)

In this case, the desired headway equals the spacing between the new follower i and the initial leader i-1. It suggests that the new follower ignores the lane changer and solely focuses on the initial leader.

- Case B: the new follower follows the lane changer ($\Phi_{B,i}(t) = x_j(t) - x_i(t)$)

Contrary to case A, case B describes a situation where the lane changer directly replaces the initial leader when it starts the anticipation process. In this scenario, the desired headway $\Phi_i(t)$ equals the spacing difference between the lane changer j and the new follower i.

Since $x_j(t) < x_{i\text{-}1}(t)$ is true for any time during the anticipation, we restrict the value of $\Phi_i(t)$ by the maximum value ($x_{i\text{-}1}(t) - x_i(t)$) and the minimum value ($x_j(t) - x_i(t)$). To better understand the changing pattern of $\Phi_i(t)$ during anticipation, we examined two examples (see Fig. 5), where the blue line represents Case A, the green line represents Case B, and the black line represents the desired headway of the new follower.

Fig. 5 **(a)** shows that the desired headway approximately superimposes with Case A at the beginning of anticipation. It suggests that most of the new follower's attention is on the initial leader. As the lateral position of the lane changer approaches the target lane, a notable trend from Fig. 5 **(a)** is that the desired headway gradually diverges from Case A and converges to Case B. This pattern indicates that the new follower gradually shifts its attention from the initial leader to the lane changer. Towards the end of anticipation, the desired headway almost overlaps with Cased B, signifying that the new follower closely follows the lane changer. In other words, the lane changer draws all the new follower's attention. Compared to Example 1, Example 2 in Fig. 5 **(b)** suggests that the lane changer indeed affects the new follower's behavior since the black line is below the blue line. However, even at the end of anticipation, the new follower does not devote all the attention to the lane changer, as evidenced by the significant difference between black and green lines. This is because the initial leader still has an effect on the new follower since the lane changer is not completely overlapped with the new

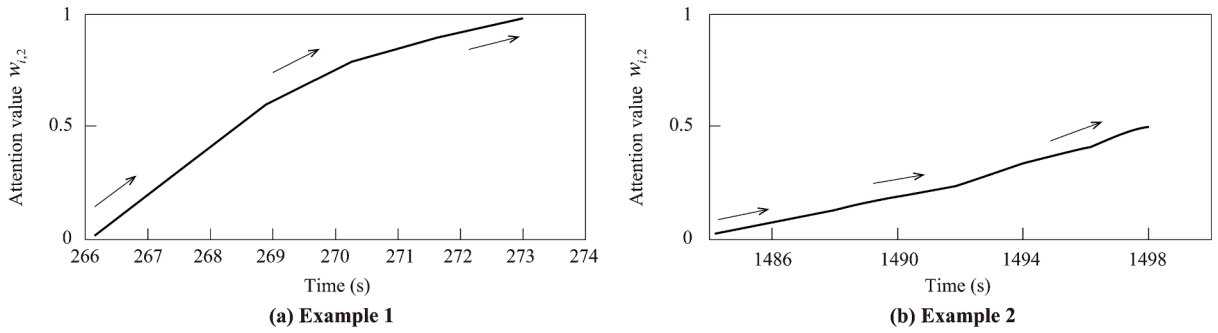

Fig. 6. The new follower's attention on the lane changer during anticipation.

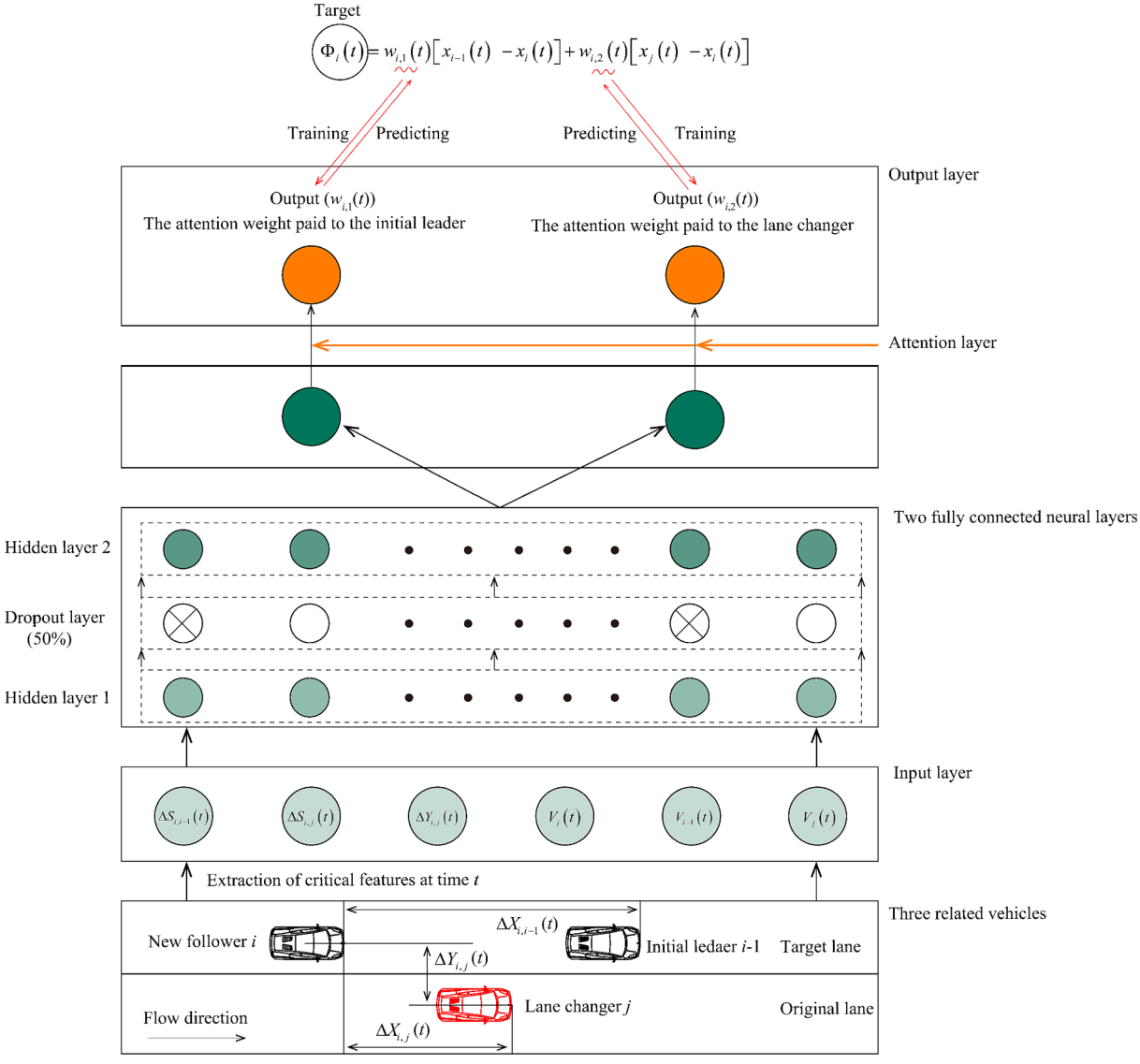

Fig. 7. The architecture of the attention neural network.

follower in the longitudinal direction. In summary, the changing process of desired headway provides insight into the extent to which the new follower is affected by the lane changer and the initial leader.

To quantify the above discussions, we introduce two attention weights: $w_{i,1}$ (t) and $w_{i,2}$ (t), representing the attention of the new follower *i* paid to the initial leader and the lane changer at time *t*, respectively. Recall that we assume only the initial leader and the lane changer affect the new follower. Thus, $w_{i,1}$(t) plus $w_{i,2}$ (t) equals 1. The desired headway Φ_i (t) can be rewritten as follows:

$$\Phi_i(t) = w_{i,1}(t)[x_{i-1}(t) - x_i(t)] + w_{i,2}(t)[x_j(t) - x_i(t)] \tag{6}$$

According to the real trajectory of desired leader (Φ_i (t) $= x_i(t) - x_i(t)$), these two attention weights in **Eq. (6)** can be solved as below:

$$Attention\ \ paid\ to\ the\ initial\ leader: w_{i,1}(t) = \frac{x_i(t) - x_i(t) - [x_j(t) - x_i(t)]}{x_{i-1}(t) - x_j(t)} \tag{7}$$

$$Attention\ \ paid\ to\ the\ \ lane\ changer: w_{i,2}(t) = \frac{x_i(t) - x_i(t) - [x_{i-1}(t) - x_i(t)]}{x_j(t) - x_{i-1}(t)} \tag{8}$$

To illustrate the attention mechanism, we apply **Eq. (7)** to compute the new follower's attention weight for the lane changer at each time step in the two examples presented in Fig. 5. The attention weights are plotted in Fig. 6. From Fig. 6**(a)**, we observe an increasing trend in the attention weight from 0 to 1, which is consistent with the analysis in Fig. 5 **(a)**. In Fig. 6 **(b)**, the new follower's attention to the lane changer increases but reaches a maximum value of around 0.5. It indicates that the lane changer does not capture all of the new follower's attention, which coincides with the explanation of Fig. 5 **(b)**. It follows that the time series of $w_{i,2}$ (t) (or $w_{i,1}$ (t)) can be interpreted as the attention allocated to the lane changer (or the initial leader) by the new follower during anticipation.

3.3. The architecture of the attention neural network

As stated in Section 2.2, a well-trained neural network with large amounts of data can provide a powerful tool for estimating human driving behavior. In this section, we implement a neural network to predict the attention mechanism described in **Eqs. (7)** and **(8)**. Given that these equations represent the new follower's attention towards two targets (the initial leader and the lane changer), we further add an attention layer in the neural network. Previous studies have demonstrated the successful application of attention layers in neural networks across various domains, resulting in improved learning performance when a subject allocates its attention to multiple targets (Cheng et al., 2018; Galassi et al., 2021; Wang et al., 2020). The conceptual architecture of this network is illustrated in Fig. 7.

The input features for the neural network are determined based on the interactions among the new follower, the initial leader, and the lane changer. Specifically, three commonly used factors are considered to reflect the impact of the initial leader on the new follower: the speed of the initial leader ($v_{i\text{-}1}(t)$), the speed of the new follower ($v_i(t)$), and the space headway between the initial leader and the new follower ($\Delta X_{i,i\text{-}1}$ (t)). To determine the impact of the lane changer, we select the speed of the lane changer ($v_j(t)$), the longitudinal distance between the lane changer and the new follower ($\Delta X_{i,j}$ (t)), and the lateral distance between the lane changer and the new follower ($\Delta Y_{i,j}$ (t)) (Ali et al., 2018; Gu et al., 2019; van Beinum et al., 2018). Therefore, the input vector at time *t* is denoted as Z_i (t):

$$Z_i(t) = \{\Delta X_{i,i-1}(t), \Delta X_{i,j}(t), \Delta Y_{i,j}(t), v_{i-1}(t), v_i(t), v_j(t)\} \tag{9}$$

As illustrated in Fig. 7, a two-layer of fully connected neural network is employed to score the attention value. The parameters in these two layers are shared with each other. A dropout layer is added to avoid the over-fitting problem. The outputs for the first layer ($A_i^{(1)}(t)$) and the second layer ($A_i^{(2)}(t)$) are expressed in **Eqs. (10)** and **(11)**, respectively.

$$A_i^{(1)}(t) = f\left(\mathrm{W}^{(1)} Z_i(t) + \mathrm{b}^{(1)}\right), \tag{10}$$

and

$$A_{i,p}^{(2)}(t) = f\left(\mathrm{W}^{(2)} A_i^{(1)}(t) + \mathrm{b}^{(2)}\right). \tag{11}$$

where $\mathrm{W}^{(1)}$ and $\mathrm{b}^{(1)}$ are the weight matrix and the bias vector for the first layer, $\mathrm{W}^{(2)}$ and $\mathrm{b}^{(2)}$ are the weight matrix and the bias vector for the second layer, and f(•) is the activation function. ReLU is employed as the activation function due to its effectiveness in neural networks.

The subscript *p* in **Eq. (11)** is the cell number for the output. Since it has been assumed that only the initial leader and the lane changer share the new follower's attention, *p* equals 2. Then $A_{i,p}^{(2)}(t) = \left\{A_{i,1}^{(2)}(t), A_{i,2}^{(2)}(t)\right\}$, where $A_{i,1}^{(2)}(t)$ and $A_{i,2}^{(2)}(t)$ are the scores of the importance of the initial leader and the lane changer to the new follower at time *t* regarding the input Z_i (t), respectively.

Following the standard setting of the attention layer, the score vector $A_{i,p}^{(2)}(t)$ is normalized using the *softmax* function to obtain the final attention weight vector $\widehat{w}_{i,p}(t) = \{\widehat{w}_{i,1}(t), \widehat{w}_{i,2}(t)\}$ as follows:

$$\widehat{w}_{i,1}(t) = \frac{\exp\left(A_{i,1}^{(2)}(t)\right)}{\exp\left(A_{i,1}^{(2)}(t)\right) + \exp\left(A_{i,2}^{(2)}(t)\right)}, \tag{12}$$

and

$$\widehat{w}_{i,2}(t) = \frac{\exp\left(A_{i,2}^{(2)}(t)\right)}{\exp\left(A_{i,1}^{(2)}(t)\right) + \exp\left(A_{i,2}^{(2)}(t)\right)}, \tag{13}$$

where $\widehat{w}_{i,1}(t)$ and $\widehat{w}_{i,2}(t)$ are the predicted attention weights of the new follower on the initial leader and the lane changer, respectively.

Eqs. (7) and (8) can be used with a given trajectory sample to calculate the real attention weights. The training process is treated as a regression task with the goal of minimizing the mean square error (MSE) between the real values ($w_{i,1}(t)$, $w_{i,2}(t)$) and the predicted values ($\widehat{w}_{i,1}(t)$,$\widehat{w}_{i,2}(t)$) on the training dataset D. The objective function is formulated as:

$$MSE = \sum_{\left(w_{i,1}(t),w_{i,2}(t)\right)\in D} \left[\left(w_{i,1}(t) - \widehat{w}_{i,1}(t)\right)^2 + \left(w_{i,2}(t) - \widehat{w}_{i,2}(t)\right)^2\right] \tag{14}$$

3.4. The new CF model

The attention neural network introduced in Section 3.3 provides us with the predicted new follower's attention on the initial leader and the lane changer at one specific moment t. Using this predicted attention mechanism, the predicted desired headway can be calculated via **Eq. (6)**, and the congested moving term in **Eq. (1)** can be subsequently rewritten as follows.

$$\Delta S(t) = \widehat{w}_{i,1}(t)\left[x_{i-1}(t) - x_i(t)\right] + \widehat{w}_{i,2}(t)\left[x_j(t) - x_i(t)\right] - d \tag{15}$$

Eqs. (1) and (15) lead to a new CF model, abbreviated as CF_Attention. The simulation procedures of CF_Attention are proposed in the following steps:

Step 1 defining the input vector for the attention neural network

To predict the trajectory of the new follower, we first need to determine the new follower's speed and location information at the start moment of anticipation ($t = 0$). As the trajectories of the initial leader and the lane changer during the anticipation are known, the input vector $Z_i(0)$ can be computed based on the real location and speed information of the initial leader, the lane changer, and the new follower. If the simulation time t is larger than 0, then the input vector $Z_i(t)$ can be computed based on the predicted location and speed information of the new follower $(x_i^{pred}(t),\ v_i^{pred}(t))$, and the real location and speed value of the initial leader $(x_i^{real} - 1(t),\ v_i^{real} - 1(t))$ and the lane changer $(x_j^{real}(t),\ v_j^{real}(t))$.

Step 2: Computing the desired headway of the new follower

Using the trained attention neural network and the input vector $Z_i(t)$ determined in step 1, we can obtain the predicted attention weights at time t for the initial leader $\widehat{w}_{i,1}(t)$ and the lane changer $\widehat{w}_{i,2}(t)$. Then, based on **Eq. (6)**, we can compute the predicted desired headway $\Phi_i(t)$.

Step 3: Predicting the new follower's trajectory

With the desired headway $\Phi_i(t)$ in hand, the location of the new follower i at the next time step $t + \tau$ can be calculated by solving **Eqs. (1) and (15)**. If the simulation time t is less than T_e, we return to step 1. Otherwise, we can stop this procedure since we have the entire predicted trajectory of the new follower.

To quantify the simulation error, we used the time series error indicator as computed by **Eq. (16)**

$$A(t) = x_i^{pred}(t) - x_i^{real}(t) \tag{16}$$

where *xpred i*(*t*) and *xreal i*(*t*) are the predicted location and actual location of the new follower i at time t, respectively. To provide a more comprehensive evaluation of the predicted trajectory, we adopt the Root Mean Square Error (RMSE) as a metric, which is computed as below:

$$RMSE = \sqrt{\frac{1}{n}\sum_{t=1}^{n}\left(A(t)\right)^2} \tag{17}$$

where n is the number of time steps.

3.5. CF models investigated

To verify the effectiveness of the proposed CF_Attention, three widely accepted CF models are selected for comparison. The first one is the basic Newell CF model (CF_Newell), which is able to describe the new follower's driving behavior without considering the impact of anticipation. However, the lane changer may force the new follower to decelerate to provide a larger space for its insertion (Hidas, 2002). The second model we compared is a modified version of CF_Newell, which captures the new follower's deceleration behavior. It

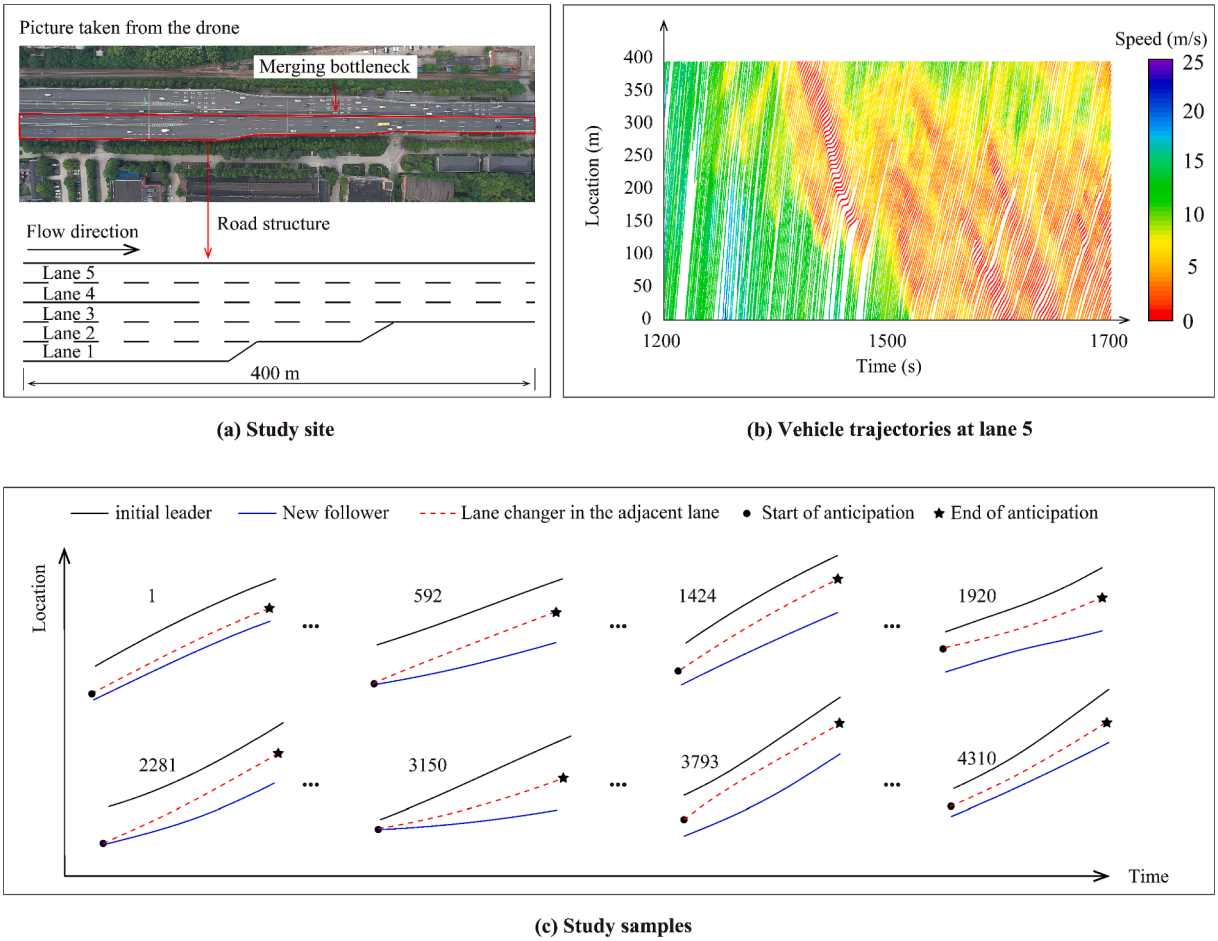

(a) Study site

(b) Vehicle trajectories at lane 5

(c) Study samples

Fig. 8. Study site and empirical data.

is abbreviated as CF_Hidas. A detailed description of the CF_Hidas is provided in Appendix A. The third model we compared against is a notable CF model proposed by Laval and Leclercq (2008) (abbreviated as CF_LL). The CF_LL is known for its ability to reproduce the deviation behavior of the new follower caused by the lane changer. The detailed formulation and calibration of the CF_LL are presented in Appendices B and C, respectively.

4. Empirical data

A period of four hours of drone videos was recorded at a merging bottleneck in Nanjing, China, on July 7th, 2021, from 8:00 am to 12:00 pm, under sunny weather with good lighting. The video recording was conducted at a height of 300 m, covering approximately a 400 m road segment. Fig. 8 **(a)** shows the structure of the study site. The traffic condition was congested during the recording, and the average vehicle speed was 6.5 m/s. The vehicle-level trajectories were automatically extracted from these drone videos. Detailed information regarding the trajectory extraction procedure can be found in our previous studies (Chen et al., 2021; Wan et al., 2020). After rectifying and filtering the original data, 24,289 vehicle trajectories were obtained. Each trajectory has a time interval of 0.03 s, including speed (m/s), location (m), acceleration (m/s^2), and lane number. An example of vehicles' trajectory in a single lane is shown in Fig. 8 **(b)**. These trajectories in Fig. 8 **(b)** are colored by the instantaneous speed, and the speed bar is displayed on the right.

The dynamic time-warping algorithm has been widely used to calibrate the element parameters in the CF_Newell model (Meng et al., 2021; Przybyla et al., 2015; Taylor et al., 2015). Here, we adopt this method to calculate τ and d for all the sampled vehicles, and the average values of τ (1.4 s) and d (6.2 m) are employed for this study.

Recall that we aim to explore the impact of anticipation. Thus, only the trajectories of the lane changer, the initial leader, and the new follower during the anticipation process are helpful. To pick up this paired sample from the entire trajectory dataset, we follow three criteria below:

(1) The start moment of anticipation is located as the lateral shift point of the lane changer, denoted as T_s. The wavelet transform algorithm is applied in this study to determine this time point, as suggested by Yang et al. (2019b) and Chen et al. (2021).

(2) The end moment of anticipation, denoted as T_e, is located once the center of the lane changer reaches the target lane edge.

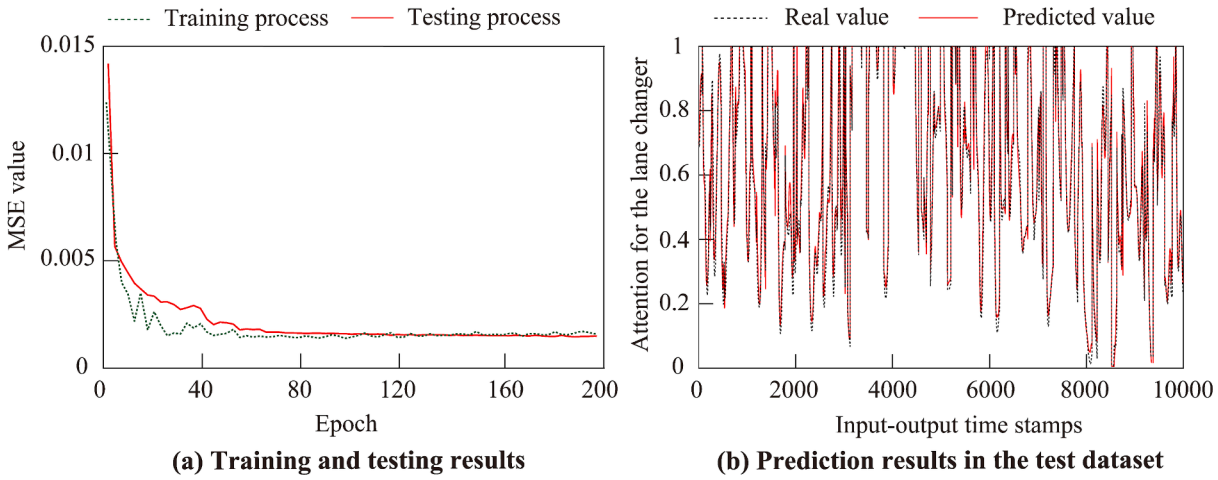

Fig. 9. Performance of the neural network with an attention layer.

(3) During the anticipation process, only the trajectory sample where the initial leader and the new follower in the target lane are the same vehicles without another LC maneuver are selected. This criterion, to a larger extent, ensures our earlier assumption. That is, the new follower is only affected by the initial leader and the lane changer.

Using these criteria, we extract 4,310 pairs of study samples. Fig. 8 **(c)** illustrates some of these study samples.

5. Performance of attention neural network

The rationality of the CF_Attention should come from the high accuracy of the attention neural network. Therefore, this section presents the training and test results of this network. 70% of the study samples are used for training. Since the trajectory's time interval in our database is 0.03 s, 748,952 time stamps are obtained for the training. Then, the input $Z_i(t)$ and the real output ($w_{i,1}(t)$ and $w_{i,2}(t)$) can be calculated at each time stamp. During training, the batch size is set to 32. The gradient descent algorithm called Adam is adopted for the primary neural networks. The learning rate is set to 0.001. The remaining 30% of the study samples form the test dataset. Similar to the training process, we obtain 1293 study samples and 302,451 input–output time stamps from the test dataset.

Fig. 9 **(a)** shows the loss curves of the training and test processes. The training curve is nearly flat after 80 epochs, indicating that the attention neural network has converged. At the same time, the testing curve is also leveled and reaches a relatively small MSE value of 0.0015. To intuitively understand the performance of the attention neural network, the plots of the real and predicted values of 10,000 input–output samples in the testing dataset are presented in Fig. 9 **(b)**. We observe a near-perfect match, indicating that the proposed attention neural network performs well in predicting the attention mechanism. The high accuracy of the attention neural network allows us to test the performance of the CF_Attention model in the following section.

6. Numerical experiments

In this section, we design three simulation experiments to test the performance of the CF_Attention. The first experiment aims to investigate how the CF_Attention works on predicting the new follower's trajectory. The second experiment evaluates whether the CF_Attention can reproduce the speed-space relationship of the new follower. The third experiment is designed to find a more accurate way to predict the oscillation caused by anticipation. The results of these three experiments are presented in Section 6.2. For each experiment, we also compare the simulation results of the CF_Attention with the three investigated CF models discussed in Section 3.5.

6.1. Simulation experiments

6.1.1. Experiment 1: The trajectory and attention mechanism

We design Experiment 1 in this section to examine the CF models' performance in predicting the new follower's trajectory and attention mechanism. The stability of CF models under two significant features: the new follower's heterogeneous behavior, and the anticipation duration, will also be examined in this experiment.

To gain a better understanding of the microscopic function of CF models at an individual level, we first select 4 cases for visualization. Specifically, in case 1 and case 2, we focus on the condition of short anticipation duration. Also here, we distinguish between the new follower being defensive (case 1) and aggressive (case 2) based on **Eq.(4)**. In case 3 and case 4, we focus on the condition of long anticipation duration. Similarly, we distinguish between the new follower being defensive (case 3) and aggressive (case 4).

We further split Experiment 1 into two parts based on the new follower's heterogeneous behavior and the anticipation duration to obtain more rigorous comparison results. In the first part, the study samples in the test dataset are divided into defensive and aggressive groups based on the new follower's behavior. Then, we simulate the new followers' trajectory using CF models and

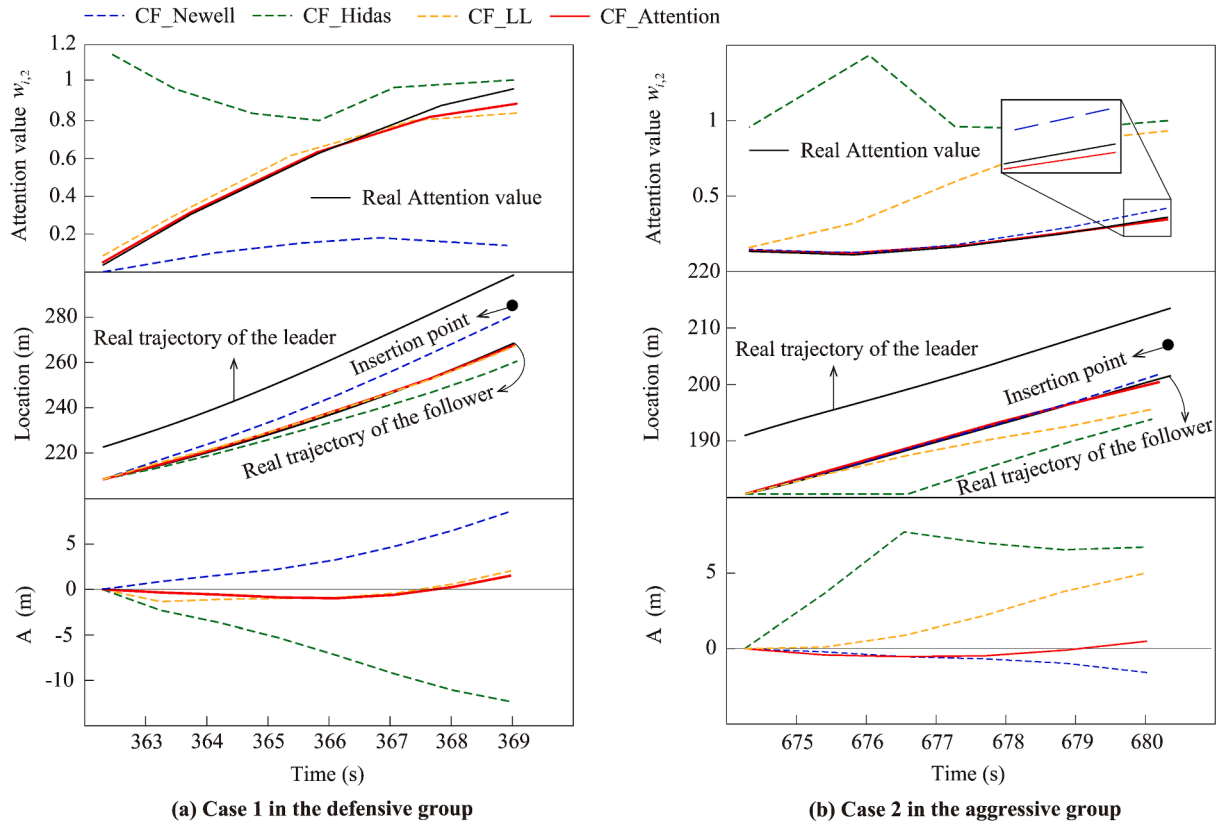

Fig. 10. Comparison between the field data and simulation results in terms of attention and trajectory under fast anticipation process condition.

calculate the RMSE (**Eq. (17)**) in each group. The comparison results allow us to check how the new follower's heterogeneous behavior affects CF models' performance.

In the second part, we investigate whether the anticipation duration affects the CF models' prediction capability. To do that, we propose 12 groups in which the duration increases from 3 s to 15 s with an interval of 1 s. Then, all the LC samples in the test dataset are allocated to these groups based on their real anticipation duration values. In each group, we simulate the new follower's trajectory by CF models and use the average RMSE to quantify the simulation error. The changing trend of the average RMSE under different groups will unveil the impact of the anticipation duration on CF models' performance.

6.1.2. Experiment 2: The speed-space relationship

In Experiment 2, we attempt to get insight into the accuracy of CF models in predicting the new follower's speed-spacing relationship. Since this relationship is in two dimensions, we hence use the Root Mean Square Percentage Error (RMSPE) to quantify the reproduction accuracy. The RMSPE can be calculated using the following equation:

$$RMSPE = \sqrt{\frac{1}{n}\sum_{t=1}^{n}\left[\frac{x_i^{pred}(t) - x_i^{real}(t)}{x_i^{real}(t)}\right]^2 + \left[\frac{v_i^{pred}(t) - v_i^{real}(t)}{v_i^{real}(t)}\right]^2} \tag{18}$$

where $v_i^{pred}(t)$ *and* v_i^{real} are the predicted and real speeds of the follower i, respectively. A lower RMSPE represents a better prediction result.

We simulate the speed-space patterns of new followers in the test dataset using CF models and calculate their RMSPE values. An ANOVA test is conducted to determine whether the mean RMSPE value of the CF_Attention is significantly different from those of other investigated CF models. Furthermore, we calculate the distribution of RMSPE values for CF models from 0 to 100%, with a 10% interval. The comparison of distributions allows us to understand the source of errors.

6.1.3. Experiment 3: The oscillation

Traffic oscillation has been widely studied in the literature because of its negative impact on traffic streams (Li et al., 2010). LC has been commonly identified as a trigger for oscillation formulation (Makridis et al., 2020). Referring back to Fig. 2, we observe that the oscillation can be amplified and formed during anticipation. Thus, we design Experiment 3 to investigate how to simulate this oscillation more accurately.

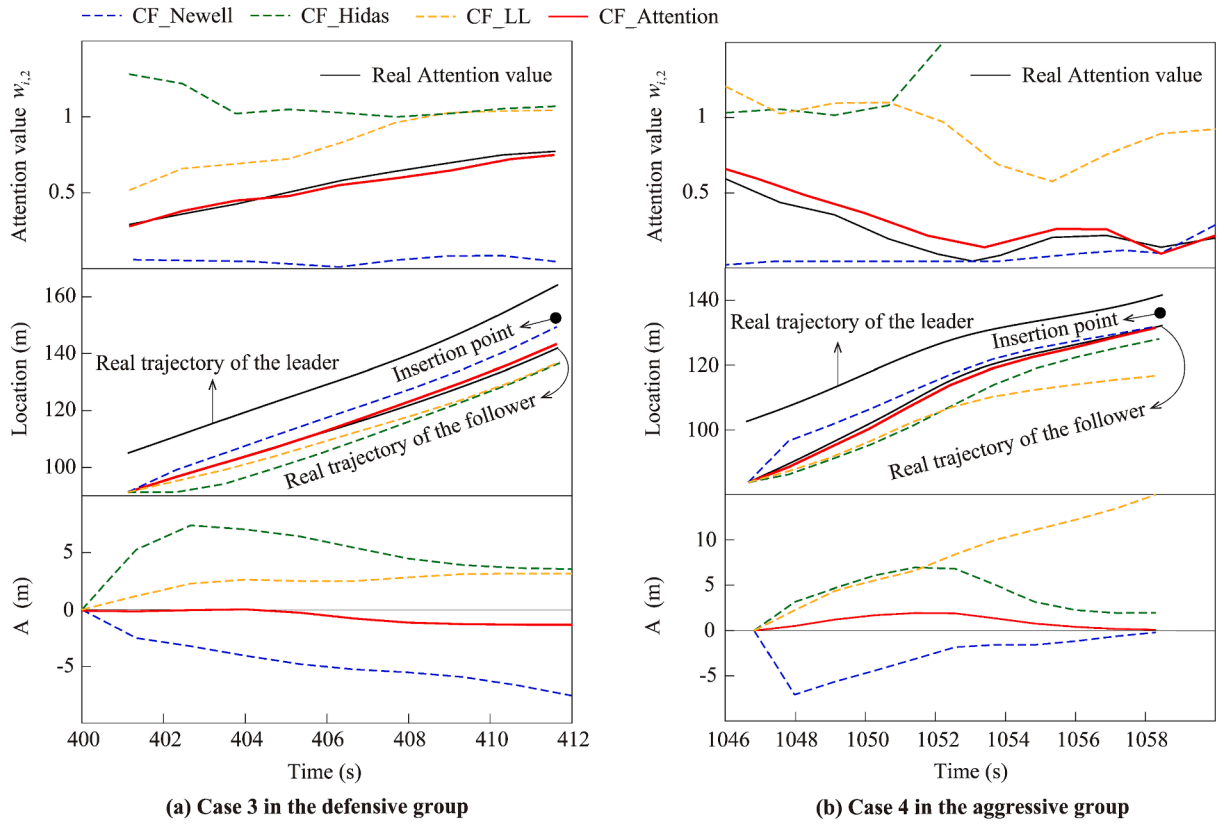

Fig. 11. Comparison between the field data and simulation results in terms of attention and trajectory under long anticipation process condition.

Three criteria are used to obtain suitable oscillations from the test trajectory dataset: a notable oscillation induced by anticipation can be observed, no other LC occurs in the oscillation, and at least five vehicles should be involved. Based on these criteria, we select 35 oscillation samples for this experiment. Then, we simulate each oscillation with the following two steps:

(1) We apply four CF models (CF_Newell, CF_Hidas, CF_LL, and CF_Attention) to predict the trajectory of the new follower, which obtained four simulations.

(2) At each simulation, the CF_Newell is used to simulate the remaining vehicles in the oscillation.

By following the above simulation steps, we create four combinations: (1) CF_Newell + CF_Newell, (2) CF_Hidas + CF_Newell, (3) CF_LL + CF_Newell and (4) CF_Attention + CF_Newel. The average value of RMSE for all vehicles in the oscillation (ARMSE) is applied to quantify the prediction error. An ANOVA test is adopted to check the statistical difference of the mean ARMSE among the 35 oscillation samples across the four combinations. Experiment 3 not only aims to find the best way to replicate the oscillation but also highlights the importance of the first driver who reacts to the disturbance.

6.2. *Experimental results*

6.2.1. *Results of Experiment 1*

Fig. 10 illustrates the simulation results regarding the new follower's attention weight, trajectory, and time series error in case 1 and case 2. The blue, green, yellow, red, and black lines represent the outcomes of CF_Newell, CF_Hidas, CF_LL, CF_Attention, and the real condition. As shown in Fig. 10, the CF_Newell exhibits a large error in case 1 while matching well with the real values in case 2. The results indicate that the CF_Newell's accuracy will be higher if the new follower is not affected by anticipation and vice versa. The CF_LL yields opposite results compared to the CF_Newell, producing smaller prediction errors in case 1 than in case 2. This is because a fixed relaxation parameter in the CF_LL assumes that the new follower is more likely to keep a large space with its leader. As a result, when the new follower maintains its original driving behavior during anticipation, the new follower's trajectory produced by the CF_LL may deviate from the actual trajectory. For the CF_Hidas, the predicted trajectories in case 1 and case 2 both exhibit significant lags from the real ones. This finding suggests that an unrealistic speed change is more likely to be induced if we directly set the lane changer as the new follower's leader at the beginning of anticipation. It is consistent with the work of Keane and Gao (2021). The red lines in Fig. 10 reveal that the CF_Attention generates more consistent results with the ground truth for the new follower's attention and trajectory in both case 1 and case 2 than other CF models.

Next, we focus on exploring the CF models' ability when the lane changer takes a long anticipation process. Fig. 11 illustrates the

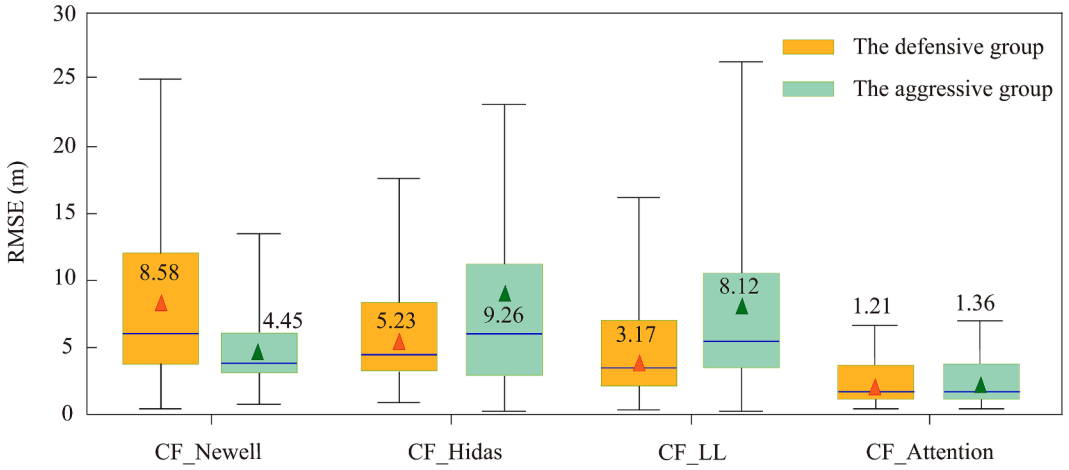

Fig. 12. The error boxes of CF models under defensive and aggressive groups.

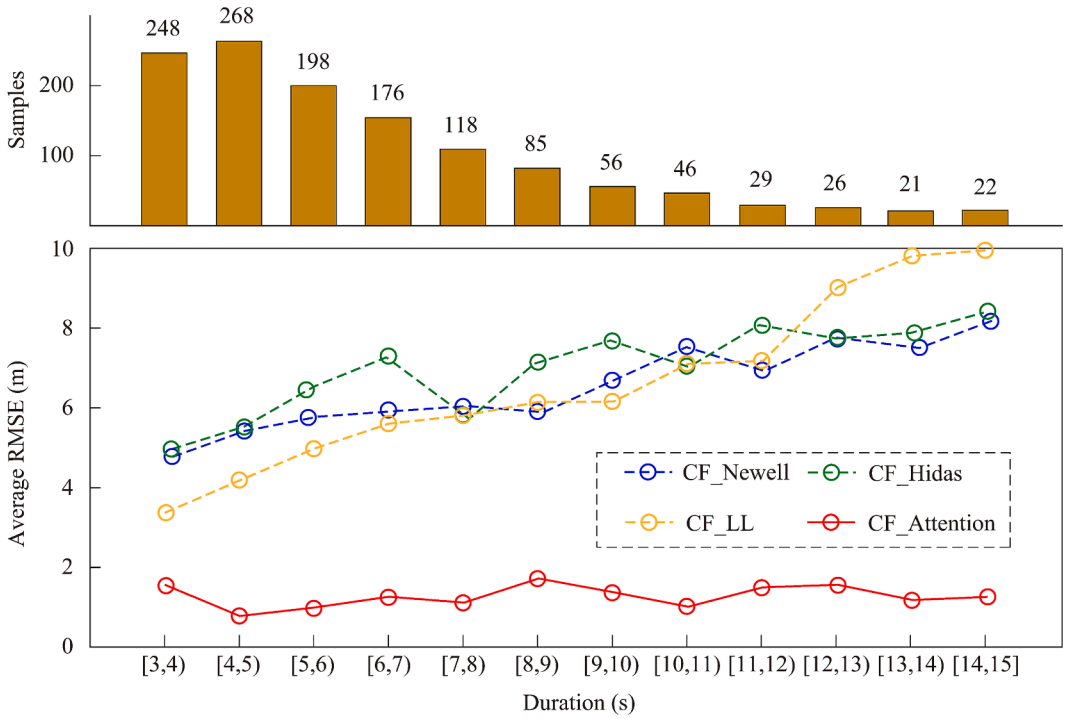

Fig. 13. The error box plot for CF models under the different duration of anticipation.

simulation results using CF models for case 3 and case 4. The CF_Attention outperforms all the other investigated models, which can be inferred by it having the closest prediction results to the real values. More importantly, based on these similar observations, we conclude that a better prediction of the attention mechanism yields a higher prediction accuracy of the new follower's trajectory.

To further verify the rigor of the above results, Fig. 12 shows the prediction error boxes of each CF model for both defensive and aggressive groups. Our results reveal a significant difference in the average RMSE between the two groups for each investigated CF model. Specifically, the CF_Newell appears more suitable for defensive new followers, while the CF_Hidas and the CF_LL are more fitting for aggressive new followers, which aligns with the analysis of Fig. 10 and Fig. 11. Notably, the CF_Attention exhibits the smallest mean RMSE values in the aggressive group (1.36 m) and the defensive group (1.21 m) compared to the other three investigated CF models. These results demonstrate that the CF_Attention yields the highest accuracy in predicting trajectories and exhibits stable performance when the new follower's behavior is heterogeneous.

Fig. 13 illustrates the impact of anticipation duration on the prediction error of CF models. We find that the error of these three investigated CF models increases with the increase in anticipation duration. The nearly unchanged trend of the red line in Fig. 13

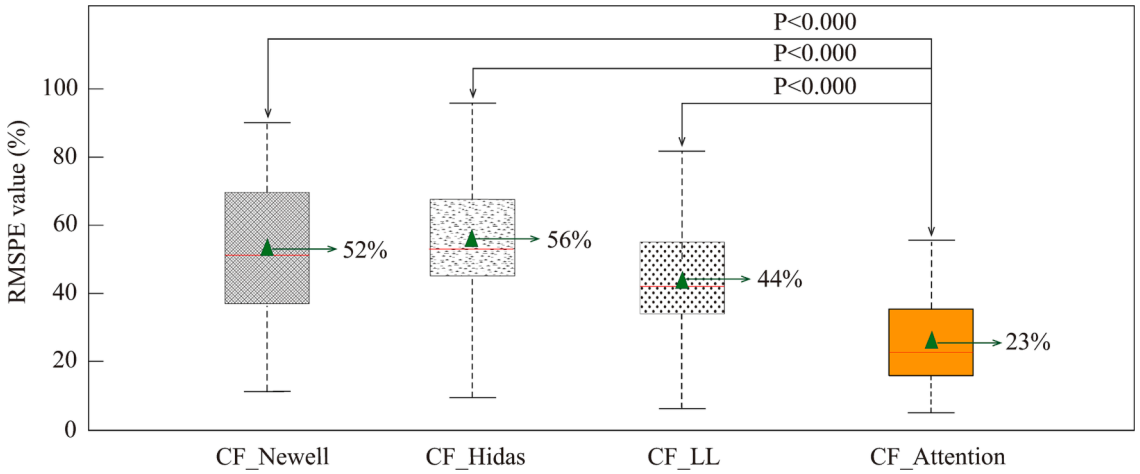

Fig. 14. ANOVA test result.

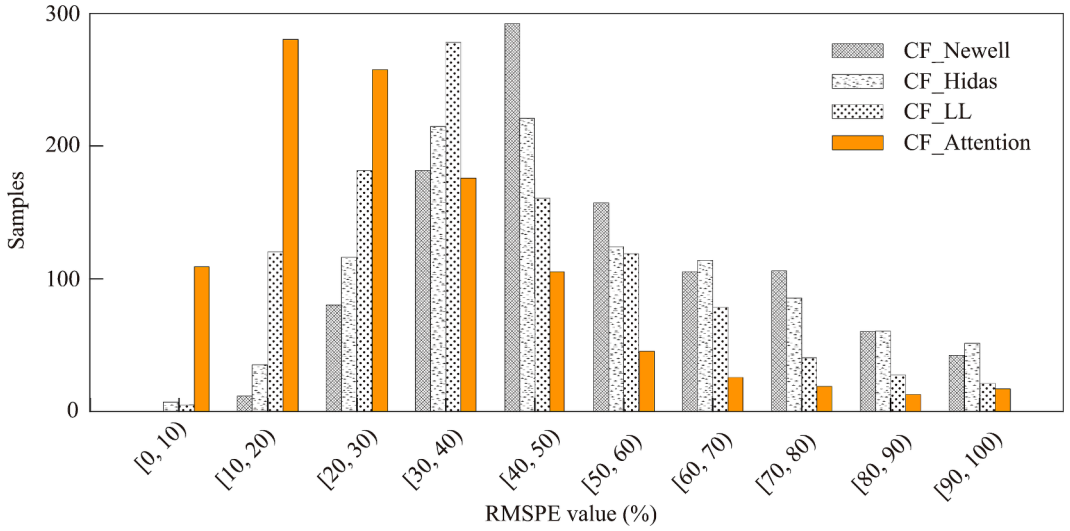

Fig. 15. RMSE distributions of the speed-space pattern.

indicates that the CF_Attention has strong robustness under different anticipation durations. Additionally, the CF_Attention shows the lowest error for each duration interval compared to the other investigated CF models.

6.2.2. Results of Experiment 2

Fig. 14 displays the ANOVA test results. It shows that the CF_Attention produces significance smaller errors in predicting the speed-space pattern (mean RMSPE = 23%) compared to the CF_Newell (mean RMSPE = 52%), the CF_Hidas (mean RMSPE = 56%) and the CF_LL (mean RMSPE = 44%). Fig. 15 gives a closer view of the RMSPE distributions for different CF models. The majority of the RMSPE values produced by the CF_Attention are concentrated between 10% and 30%, while those produced by the other three investigated CF models are concentrated between 30% and 50%.

Although RMSPE values are useful for comparing the performance across CF models, they may not provide an intuitive understanding of errors. To address this issue, we select six representative cases from the first six ranges and visually illustrate the predicted and actual values in Fig. 16. This figure helps to establish a link between the RMSPE value and the matching degree between the predicted speed-space pattern and the ground truth. Specifically, Fig. 16 **(e)** shows that the predicted pattern exhibits a significant and unaccepted error when the RMSPE value exceeds 40%. In this study, we set a threshold of 40% for the RMSPE value to roughly evaluate the performance of the CF model. We find that approximately 67% of samples' RMSPE predicted by the CF_Attention are below the 40% threshold. However, only 20%, 28%, and 40% of samples' RMSPE predicted by the CF_Newell, the CF_Hidas, and the CF_LL meet the threshold, respectively. In summary, the presented results above demonstrate that the CF_Attention outperforms all other investigated CF models in predicting the speed-space pattern.

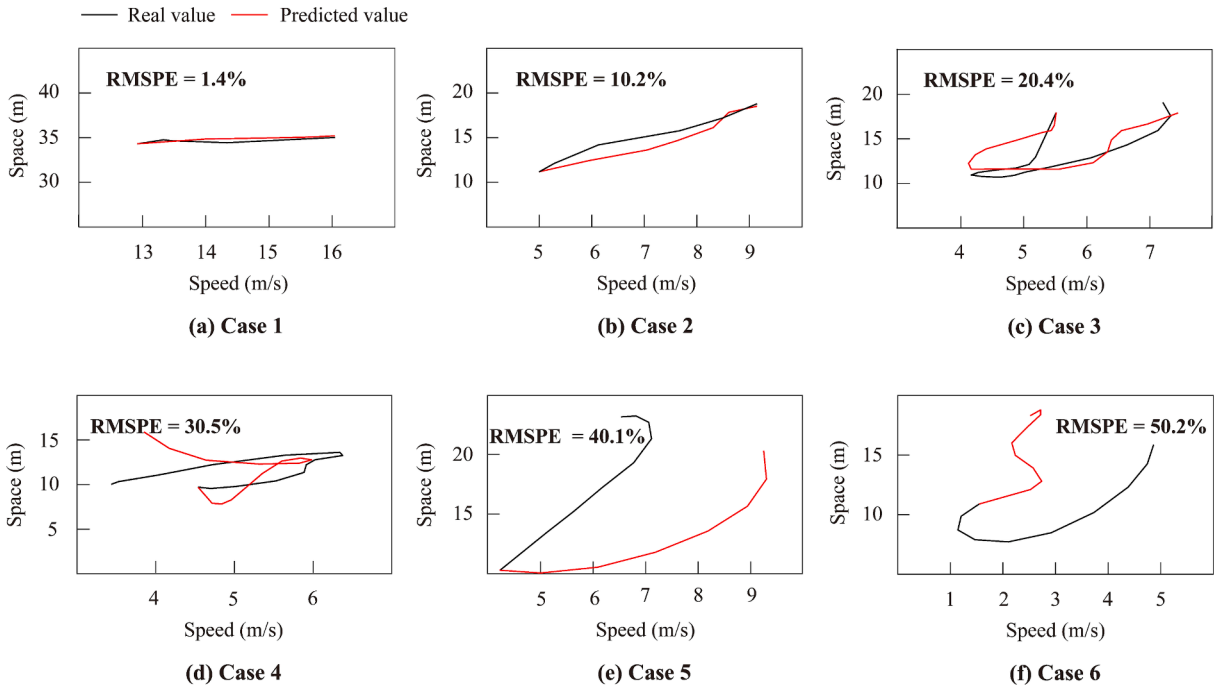

Fig. 16. A comparison of speed-spacing pattern between the simulated results and the real data under six cases.

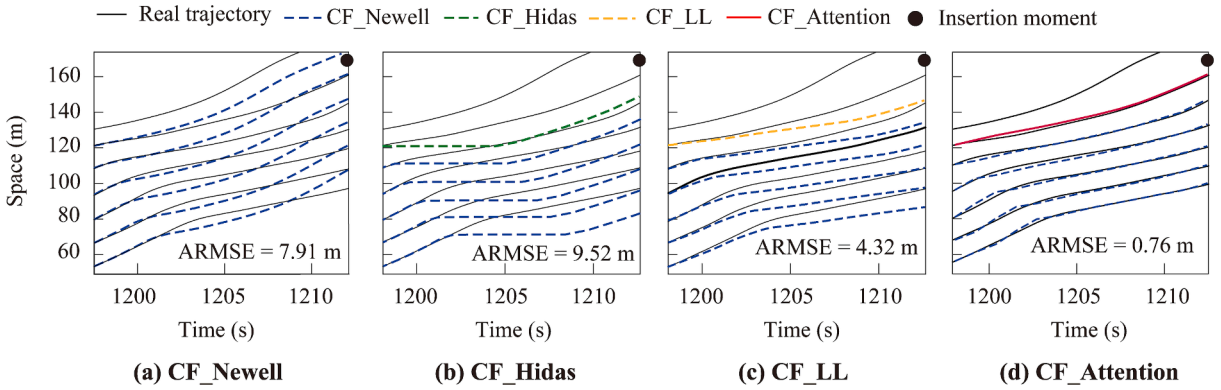

Fig. 17. A comparison of the formation of oscillation between the simulated results and real data.

Table 1
Average ARMSE for four combinations on 35 oscillation samples.

Simulation combinations	ARMSE (m)	
	Mean	S.D.
CF_Newell + CF_Newell	8.98	3.14
CF_Hidas + CF_Newell	6.51	2.85
CF_LL + CF_Newell	4.12	2.13
CF_Attention + CF_Newell	1.24	0.58

6.2.3. *Results of Experiment 3*

We first chose one oscillation sample out of the 35 oscillation samples to appreciate how the four combinations mentioned in Experiment 3 work. The black lines in Fig. 17 represent the real trajectories of this oscillation. In this case, the lane changer starts the anticipation at around 1200 s and inserts into the target lane at around 1212 s. During the 12 s period of anticipation, the first vehicle continues to accelerate while its immediate follower decelerates due to the impact of anticipation. We use these four combinations to

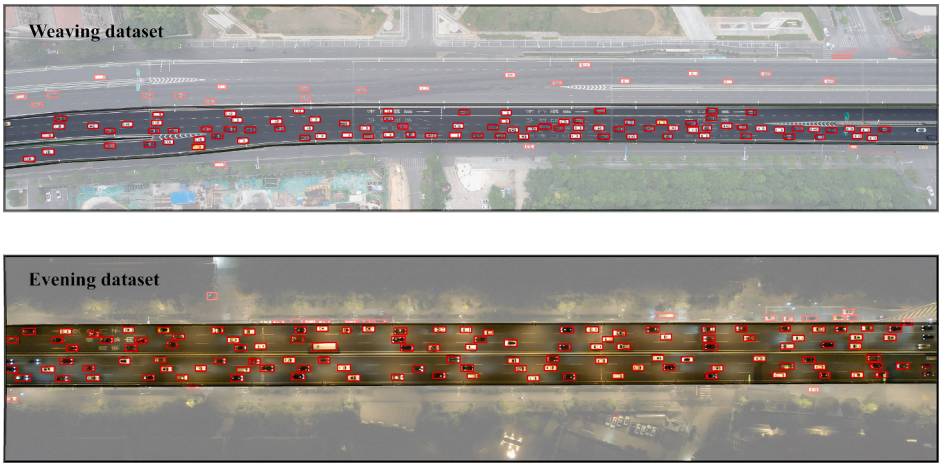

Fig. 18. Two additional datasets for the transferability test.

Table 2
Test results of the transferability of the CF_Attention.

Experiments	Error indicator	Original dataset		Weaving dataset		Evening dataset	
		Mean	S.D.	Mean	S.D.	Mean	S.D.
Experiment 1							
Defensive behavior	RMSE (m)	**1.21**	**0.34**	1.43	0.42	0.9	0.29
Aggressive behavior	RMSE (m)	**1.36**	**0.38**	1.55	0.37	1.04	0.31
Duration	RMSE (m)	**1.27**	**0.29**	1.49	0.32	0.97	0.27
Experiment 2							
Speed-space relationship	RMSPE (%)	**23.24**	**7.22**	28.52	8.52	19.71	5.23
Experiment 3							
Oscillation	ARMSE (m)	**1.24**	**0.21**	1.37	0.29	1.18	0.16

simulate this oscillation, and the simulation results are also shown in Fig. 17.

Fig. 17 **(a)-(c)** shows that the new follower's trajectories predicted by the CF_Newell, the CF_Hidas, and the CF_LL considerably deviate from the actual trajectory. Meanwhile, significant errors are observed when we directly use the simple CF_Newell model to predict the remaining vehicles' trajectories. Contrarily, in Fig. 17 **(d)**, the CF_Attention produces a fairly good trajectory of the new follower, almost overlapping with the actual value. Therefore, the entire oscillation can be predicted with a small error (ARMSE = 0.76 m) using the CF_Newell. This result is reasonable because the behavior of the following vehicle in the oscillation is mainly restricted by its leader. Thus, the higher prediction accuracy of the first vehicle that encounters the disturbance leads to better prediction of the entire oscillation. Table 1 compares the mean ARMSE for the 35 oscillation samples simulated by the four combinations. The ANOVA test results indicate that the mean ARMSE value simulated by the combination of CF_Attention + CF_Newell is significantly smaller than the other combinations. It demonstrates that the oscillation can be well replicated using our new CF model to predict the new follower's trajectory and the CF_Newell to predict the rest of the vehicles' trajectories.

7. Transferability test

In order to further examine the transferability of the proposed CF_Attention, in this section, we directly implement this new model without retraining on two new trajectory datasets. The first trajectory dataset was collected at a weaving bottleneck on Thursday, May 21st, 2021, from 8:30 am to 9:30 am (morning peak), namely the weaving dataset. The second trajectory dataset was collected at a basic road section on Monday, Dec. 13th, 2021, from 6:30 pm to 7:30 pm (evening peak), namely the evening dataset. The structures of these two additional sites are shown in Fig. 18. Based on the trajectory extraction and LC sample extraction methods introduced in Section 4, we obtain 1327 and 1734 LC study samples from the weaving and evening datasets, respectively. Then, we conduct experiments 1 to 3 on these two datasets only using the CF_Attention.

Table 2 presents the transferability results. It shows that the prediction errors of the CF_Attention increase for all three experiments to a reasonable extent when we apply this model to the weaving dataset. Fortunately, the simulation results of the CF_Attention for these three experiments on the evening dataset are even better than that on the original testing dataset. The above results are reasonable because the driving behavior in the weaving section is the most complicated than that in the merging section, followed by that in the basic road section. Since we only trained our model with trajectory data at a merging bottleneck, this slight increase of error in the weaving dataset is acceptable, and this better performance in the evening dataset is expected. Thus, we conclude that the

CF_Attention has good transferability to other locations and times.

8. Conclusion

Although an LC event inevitably affects the new follower's behavior in the congested flow, there has been little research on how the new follower behaves during the anticipation stage of the LC maneuver. In this study, we aim to provide new insights into this issue and integrate the anticipation impact into the CF model to improve the prediction accuracy of the new follower's trajectory. This is accomplished in two steps. Firstly, we develop two time-series variables to represent the new follower's attention on the initial leader and the lane changer. These two variables explain the desired headway that the new follower is willing to follow during anticipation. A neural network with an attention layer is established to predict these two variables. This network is trained and tested on a 4-hour trajectory dataset collected at a merging bottleneck. The result shows that new follower's attention variables can be predicted with high accuracy. Secondly, we incorporate attention variables into the Newell CF model, which yields a new CF model (CF_Attention).

We design three experiments to validate the performance of the CF_Attention and compared it to three other investigated CF models. The simulation results indicate that the CF_Attention greatly enhances the prediction accuracy of the new follower's trajectory. Then, we test the stability of CF models. The results demonstrate that the CF_Attention holds the highest accuracy even when the new follower's behavior is heterogeneous, and the anticipation duration ranges from 3 s to 15 s. Furthermore, we examine the CF models' ability to predict the speed-space pattern of the new follower during anticipation. The comparison results unveil that the CF_Attention can significantly reduce the prediction error. Interestingly, we notice that 35 oscillation samples on the test dataset are formed due to anticipation. Then, we design four combinations to replicate this kind of oscillation. The results suggest that the prediction accuracy of the oscillation is highly related to the prediction accuracy of the trajectory of the new follower. The best combination is to adopt the CF_Attention to predict the new follower's trajectory and the original Newell CF model to predict the remaining vehicles' trajectories. Finally, a transferability test concludes that the CF_Attention performs well at different locations and times.

The primary improvement of the novel CF model over the previous related CF models is its ability to predict the new follower's trajectory more accurately during the anticipation stage of the lane changer. We believe the proposed attention mechanism is promising and can be applied to other scenarios. For example, the previous studies only modeled the new follower's trajectory during relaxation, which is separated from the anticipation process. With the newly proposed modeling framework, the attention mechanism can be extended to the end of the relaxation stage. After that, a new model for the lane changer's impact during the entire LC process can be established, which can collaborate with CF models to evaluate multiple-lane traffic flow. Furthermore, once we can fully understand the LC impact and continuously model how the surrounding vehicles respond to it, the formation of some critical traffic problems, such as the oscillation and the capacity drop induced by the LC maneuver, could be unveiled. That will be tackled in our further work.

CRediT authorship contribution statement

Kequan Chen: Conceptualization, Methodology, Software, Validation, Writing – original draft. **Victor L. Knoop:** Methodology, Validation, Writing – review & editing. **Pan Liu:** Conceptualization, Funding acquisition, Supervision, Writing – review & editing. **Zhibin Li:** Validation, Writing – review & editing. **Yuxuan Wang:** Formal analysis, Investigation, Validation.

Declaration of Competing Interest

The authors declare that they have no known competing financial interests or personal relationships that could have appeared to influence the work reported in this paper.

Data availability

Data will be made available on request.

Acknowledgments

This work was supported by the National Natural Science Foundation of China (51925801, 52232012, 52272331), the Fundamental Research Funds for the Central Universities (2242019R40060, 2242020K40063). The authors thank the anonymous reviewers for their time to review our article and their constructive comments.

Appendix A. Modified Newell CF model (CF_Hidas)

Hidas (2002) suggested that the new follower will change its following mode if the lane changer in the adjacent lane forces the new follower to decelerate. We incorporate this idea into the CF_Newell. Specifically, we assume that the new follower i changes its following target from the initial leader i-1 directly to the lane changer j when a trigger appears. The trigger in this study is considered as the anticipation process. Then, the congestion term in **Eq. (1)** can be rewritten as:

$$\Delta S(t) = x_j(t) - x_i(t) - d \tag{19}$$

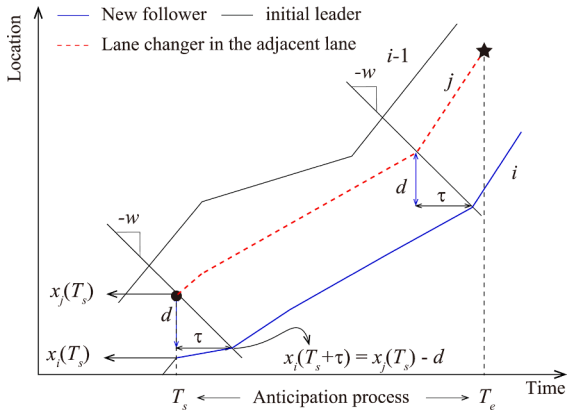

Fig. A1. Illustration of the CF_Hidas.

where x_j (t) is the location of lane changer j in the adjacent lane at time t.

Fig. A1 shows a simple example where the new follower i follows the rules of **Eq. (1)** and **Eq. (19)**. In this figure, the blue line represents the trajectory of the new follower, which is obtained by considering the lane changer as the initial leader even though it is still in the adjacent lane.

Appendix B. CF model with a relaxation parameter (CF_LL)

Laval and Leclercq (2008) proposed a microscopic CF model to describe the new follower's behavior during the relaxation process (CF_LL). Their model allows the new follower to deviate from the Newell trajectory in a determined way. Based on the statement of Zheng et al. (2013), the follower also exhibits this deviation behavior during the anticipation process. Additionally, they also suggested that the anticipation and relaxation processes can be considered one process in the relaxation model. Notice that this is only a conjecture that has not been verified yet. Therefore, we are interested in the performance of the CF_LL model in predicting the new follower's behavior during anticipation. According to the work of Laval and Leclercq (2008), the congestion term in **Eq. (1)** can be computed as below:

$$\Delta S(t) = \left[v_j(t) - \hat{v}_i(t)\right]\tau - d \tag{20}$$

where v_j (t) is the speed of the lane changer j at time t, $\hat{v}_i$ (t) is the virtual speed of the new follower i at time t. The term $\hat{v}_i$ (t) is unknown at this moment, and **Eq. (21)** can be used to predict it:

$$\hat{v}_i(t) = \Delta N_i(t) v_j(t) + (1 - \Delta N_i(t)) v_j(t+\tau) - \varepsilon \tag{21}$$

$$\Delta N_i(t) = \frac{x_j(t) - x_i(t)}{x_{i-1}(t) - x_i(t)} \tag{22}$$

The term ε in **Eq. (21)** is the relaxation parameter. It captures the follower's willingness to deviate from the equilibrium trajectory. If ε equals 0, the speed of the new follower is predicted by the CF_Newell. With the increase of ε, the new follower is more likely to accept a larger space than the equilibrium pace. Then, the CF_LL is described mathematically by **Eqs. (1)**, **(20)**, **(21)**, and **(22)**. The critical relaxation parameter in **Eq. (21)** can be calibrated as below:

$$t = \frac{v_j(T_s) + w}{\beta}\left(\exp\left[\beta \frac{1 - \Delta N_i(T)}{\varepsilon w k}\right] - 1\right) \tag{23}$$

where t is the relaxation time, β is a constant acceleration rate, and k is the congested density.

Regarding the CF_LL, a relaxation parameter needs to be additionally calibrated. In Appendix C, we will show the detailed calibration procedure for this parameter.

Appendix C. Calibration of the CF_LL

Appendix C aims to present the detailed procedure for determining the relaxation parameter ε in the CF_LL. The relaxation parameter in **Eq. (21)** allows the follower deviates to the equilibrium state. Then, the follower will take a longer time to reach

equilibrium. **Eq. (23)** represents the correlation between convergence time t and the initial condition $\Delta N_i\,(T_d)$. Thus, we have to find a suitable value of relaxation parameter ε to ensure that the convergence time and corresponding initial condition consist of the observation. Based on our trajectory dataset, the basic factors in **Eq. (23)** are determined as below.

- *Wave speed w*

  As τ and d are set as 1.4 s and 6.2 m across all drivers, the wave speed can be computed by τ/d. Then we have $w \approx 16$ km/h.

- *Acceleration rate β*

  As Laval and Leclercq (2008) and Duret et al. (2011) suggested, we set the value of β as 1 m/s^2.

- *Congested density k*

  Based on the minimum stop distance, the congested density $k \approx 161$ vehicle/km.

- *Insertion speed $v_j\,(T_e)$*

  The average value of the insertion speed for all the 4310 study samples (31 km/s) is taken as the $v_j\,(T_e)$.

- *Initial condition $\Delta N_i\,(T_d)$*

  We measure the initial condition for all the 4310 pairs at the insertion moment based on **Eq. (22)**. The average value (0.49) is set for $\Delta N_i\,(T_d)$. This value is consistent with the work of Laval and Leclercq (2008), who thought this value in their model should be close to 0.5.

- *Convergence time t*

  As mentioned in Section 4, all the 4310 study samples end at insertion. However, the convergence time in **Eq. (23)** reflects the duration of the relaxation process. To obtain the relaxation duration, we additionally considered the following trajectory of the lane changer in the target lane. Note that the lane changer who conducts another LC maneuver once it inserts in the target lane is excluded from the 4310 samples. Then, we get 3425 samples. The average value of relaxation duration across these samples ($t \approx 13$ s) is considered in this study.

Based on the above setting, we solve **Eq. (23)**. The relationship between t and $\Delta N_i\,(T_d)$ under different values of relaxation parameter ε is shown in Fig. C1. As we can see from this figure when the ε equals 3.7, the convergence time and corresponding value of $\Delta N_i\,(T_d)$ match well with the observations.

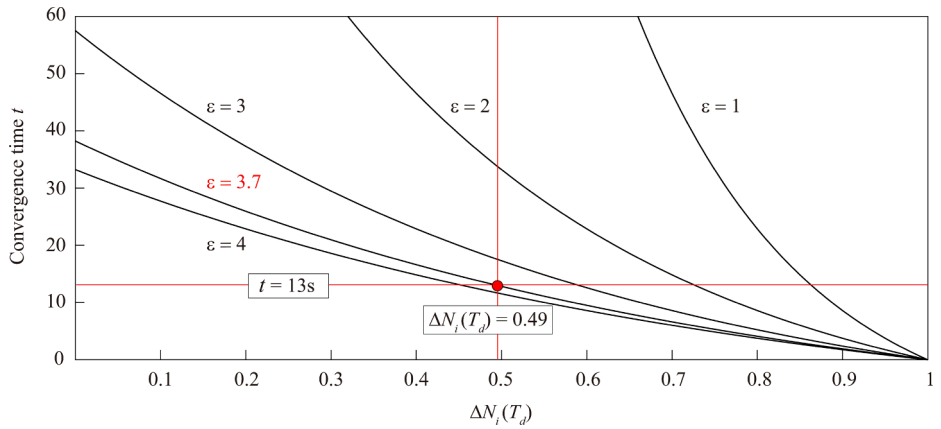

Fig. C1. The relaxation between time to convergence and $\Delta N_i\,(T_d)$ for different values of relaxation parameter ε.

References

Ali, Y., Zheng, Z., Haque, M.M., 2018. Connectivity's impact on mandatory lane-changing behaviour: evidences from a driving simulator study. Transport. Res. Part C: Emerg. Technol. 93, 292–309. https://doi.org/10.1016/j.trc.2018.06.008.

Chen, D., Laval, J., Zheng, Z., Ahn, S., 2012. A behavioral car-following model that captures traffic oscillations. Transp. Res. B Methodol. 46, 744–761. https://doi.org/10.1016/j.trb.2012.01.009.

Chen, D., Ahn, S., Laval, J., Zheng, Z., 2014. On the periodicity of traffic oscillations and capacity drop: the role of driver characteristics. Transp. Res. B Methodol. 59, 117–136.

Chen, K., Liu, P., Li, Z., Wang, Y., Lu, Y., 2021. Modeling anticipation and relaxation of lane changing behavior using deep learning. Transp. Res. Rec. 2675, 186–200.

Chen, K., Knoop, V.L., Liu, P., Li, Z., Wang, Y., 2022. How gaps are created during anticipation of lane changes. Transportmetrica B: Transport Dynamics 1–21. https://doi.org/10.1080/21680566.2022.2152129.

Cheng, Z., Ding, Y., He, X., Zhu, L., Song, X., Kankanhalli, M., 2018. Aˆ3NCF: An Adaptive Aspect Attention Model for Rating Prediction, in: Proceedings of the Twenty-Seventh International Joint Conference on Artificial Intelligence. Presented at the Twenty-Seventh International Joint Conference on Artificial Intelligence {IJCAI-18}, International Joint Conferences on Artificial Intelligence Organization, Stockholm, Sweden, pp. 3748–3754. Doi: 10.24963/ijcai.2018/521.

Chiabaut, N., Buisson, C., Leclercq, L., 2009. Fundamental diagram estimation through passing rate measurements in congestion. IEEE Trans. Intell. Transp. Syst. 10, 355–359.

Duret, A., Ahn, S., Buisson, C., 2011. Passing rates to measure relaxation and impact of lane-changing in congestion. Comput. Aided Civ. Inf. Eng. 26, 285–297.

Galassi, A., Lippi, M., Torroni, P., 2021. Attention in Natural Language Processing. IEEE Trans. Neural Netw. Learning Syst. 32, 4291–4308. https://doi.org/10.1109/TNNLS.2020.3019893.

Gu, X., Abdel-Aty, M., Xiang, Q., Cai, Q., Yuan, J., 2019. Utilizing UAV video data for in-depth analysis of drivers' crash risk at interchange merging areas. Accid. Anal. Prev. 123, 159–169. https://doi.org/10.1016/j.aap.2018.11.010.

Heesen, M., Baumann, M., Kelsch, J., Nause, D., Friedrich, M., 2012. Investigation of cooperative driving behaviour during lane change in a multi-driver simulation environment. In: in: Human Factors and Ergonomics Society (HFES) Europe Chapter Conference Touluse, pp. 305–318.

Hidas, P., 2002. Modelling lane changing and merging in microscopic traffic simulation. Transport. Res. Part C: Emerg. Technol. 10, 351–371.

Huang, Y.-X., Jiang, R., Zhang, H., Hu, M.-B., Tian, J.-F., Jia, B., Gao, Z.-Y., 2018. Experimental study and modeling of car-following behavior under high speed situation. Transport. Res. Part C: Emerg. Technol. 97, 194–215. https://doi.org/10.1016/j.trc.2018.10.022.

Keane, R., Gao, H.O., 2021. A formulation of the relaxation phenomenon for lane changing dynamics in an arbitrary car following model. Transport. Res. Part C: Emerg. Technol. 125, 103081 https://doi.org/10.1016/j.trc.2021.103081.

Laval, J.A., Daganzo, C.F., 2006. Lane-changing in traffic streams. Transp. Res. B Methodol. 40, 251–264.

Laval, J.A., Leclercq, L., 2008. Microscopic modeling of the relaxation phenomenon using a macroscopic lane-changing model. Transp. Res. B Methodol. 42, 511–522.

Lee, S., Ngoduy, D., Keyvan-Ekbatani, M., 2019. Integrated deep learning and stochastic car-following model for traffic dynamics on multi-lane freeways. Transport. Res. Part C: Emerg. Technol. 106, 360–377. https://doi.org/10.1016/j.trc.2019.07.023.

Li, M., Li, Z., Xu, C., Liu, T., 2020. Short-term prediction of safety and operation impacts of lane changes in oscillations with empirical vehicle trajectories. Accid. Anal. Prev. 135, 105345 https://doi.org/10.1016/j.aap.2019.105345.

Li, X., Peng, F., Ouyang, Y., 2010. Measurement and estimation of traffic oscillation properties. Transp. Res. B Methodol. 44, 1–14. https://doi.org/10.1016/j.trb.2009.05.003.

Ma, L., Qu, S., 2020. A sequence to sequence learning based car-following model for multi-step predictions considering reaction delay. Transport. Res. Part C: Emerg. Technol. 120, 102785 https://doi.org/10.1016/j.trc.2020.102785.

Makridis, M., Leclercq, L., Ciuffo, B., Fontaras, G., Mattas, K., 2020. Formalizing the heterogeneity of the vehicle-driver system to reproduce traffic oscillations. Transport. Res. Part C: Emerg. Technol. 120, 102803.

Meng, D., Song, G., Wu, Y., Zhai, Z., Yu, L., Zhang, J., 2021. Modification of Newell's car-following model incorporating multidimensional stochastic parameters for emission estimation. Transp. Res. Part D: Transp. Environ. 91, 102692.

Mo, Z., Shi, R., Di, X., 2021. A physics-informed deep learning paradigm for car-following models. Transport. Res. Part C: Emerg. Technol. 130, 103240 https://doi.org/10.1016/j.trc.2021.103240.

Newell, G.F., 2002. A simplified car-following theory: a lower order model. Transp. Res. B Methodol. 36, 195–205.

Ngoduy, D., Lee, S., Treiber, M., Keyvan-Ekbatani, M., Vu, H.L., 2019. Langevin method for a continuous stochastic car-following model and its stability conditions. Transport. Res. Part C: Emerg. Technol. 105, 599–610. https://doi.org/10.1016/j.trc.2019.06.005.

Przybyla, J., Taylor, J., Jupe, J., Zhou, X., 2015. Estimating risk effects of driving distraction: A dynamic errorable car-following model. Transport. Res. Part C: Emerg. Technol. 50, 117–129. https://doi.org/10.1016/j.trc.2014.07.013.

Schakel, W.J., Knoop, V.L., van Arem, B., 2012. Integrated lane change model with relaxation and synchronization. Transp. Res. Rec. 2316, 47–57.

Taylor, J., Zhou, X., Rouphail, N.M., Porter, R.J., 2015. Method for investigating intradriver heterogeneity using vehicle trajectory data: A Dynamic Time Warping approach. Transp. Res. B Methodol. 73, 59–80. https://doi.org/10.1016/j.trb.2014.12.009.

Treiber, M., Hennecke, A., Helbing, D., 2000. Congested traffic states in empirical observations and microscopic simulations. Phys. Rev. E 62, 1805–1824. https://doi.org/10.1103/PhysRevE.62.1805.

van Beinum, A., Farah, H., Wegman, F., Hoogendoorn, S., 2018. Driving behaviour at motorway ramps and weaving segments based on empirical trajectory data. Transport. Res. Part C: Emerg. Technol. 92, 426–441. https://doi.org/10.1016/j.trc.2018.05.018.

Wan, Q., Peng, G., Li, Z., Inomata, F.H.T., 2020. Spatiotemporal trajectory characteristic analysis for traffic state transition prediction near expressway merge bottleneck. Transport. Res. Part C: Emerg. Technol. 117, 102682.

Wang, W., Huang, Y., Wang, L., 2020. Long video question answering: A Matching-guided Attention Model. Pattern Recogn. 102, 107248 https://doi.org/10.1016/j.patcog.2020.107248.

Yang, M., Wang, X., Quddus, M., 2019b. Examining lane change gap acceptance, duration and impact using naturalistic driving data. Transport. Res. Part C: Emerg. Technol. 104, 317–331. https://doi.org/10.1016/j.trc.2019.05.024.

Yang, D., Zhu, L., Liu, Y., Wu, D., Ran, B., 2019a. A Novel Car-Following Control Model Combining Machine Learning and Kinematics Models for Automated Vehicles. IEEE Trans. Intell. Transport. Syst. 20, 1991–2000. https://doi.org/10.1109/TITS.2018.2854827.

Yeo, H., Skabardonis, A., Halkias, J., Colyar, J., Alexiadis, V., 2008. Oversaturated freeway flow algorithm for use in next generation simulation. Transp. Res. Rec. 2088, 68–79.

Zhang, Y., Chen, X., Wang, J., Zheng, Z., Wu, K., 2022. A generative car-following model conditioned on driving styles. Transport. Res. Part C: Emerg. Technol. 145, 103926 https://doi.org/10.1016/j.trc.2022.103926.

Zhang, X., Sun, J., Qi, X., Sun, J., 2019. Simultaneous modeling of car-following and lane-changing behaviors using deep learning. Transport. Res. Part C: Emerg. Technol. 104, 287–304. https://doi.org/10.1016/j.trc.2019.05.021.

Zheng, Z., Ahn, S., Chen, D., Laval, J., 2011. Freeway Traffic Oscillations: Microscopic Analysis of Formations and Propagations using Wavelet Transform. Procedia. Soc. Behav. Sci. 17, 702–716. https://doi.org/10.1016/j.sbspro.2011.04.540.

Zheng, Z., Ahn, S., Chen, D., Laval, J., 2013. The effects of lane-changing on the immediate follower: Anticipation, relaxation, and change in driver characteristics. Transport. Res. Part C: Emerg. Technol. 26, 367–379. https://doi.org/10.1016/j.trc.2012.10.007.

Zhou, M., Qu, X., Li, X., 2017. A recurrent neural network based microscopic car following model to predict traffic oscillation. Transport. Res. Part C: Emerg. Technol. 84, 245–264. https://doi.org/10.1016/j.trc.2017.08.027.

Zhu, M., Wang, X., Wang, Y., 2018. Human-like autonomous car-following model with deep reinforcement learning. Transport. Res. Part C: Emerg. Technol. 97, 348–368. https://doi.org/10.1016/j.trc.2018.10.024.